bioRxiv preprint doi: https://doi.org/10.1101/073189; this version posted September 3, 2016. The copyright holder for this preprint (which was not certified by peer review) is the author/funder. All rights reserved. No reuse allowed without permission.

A Novel Clustering Method for Patient Stratification

Hongfu Liu[1*], Rui Zhao[2,3*], Hongsheng Fang[2,3,4], Feixiong Cheng[5,6], Yun Fu[1,7] & Yang-Yu Liu[2,6]

[1]*Department of Electrical and Computer Engineering, Northeastern University, Boston, Massachusetts 02115, USA.*

[2]*Channing Division of Network Medicine, Brigham and Women's Hospital, Harvard Medical School, Boston, Massachusetts 02115, USA.*

[3]*Chu Kochen Honors College, Zhejiang University, Hangzhou, Zhejiang 310058, China.*

[4]*Department of Statistics, Stanford University, Stanford, California 94305, USA.*

[5]*Center for Complex Network Research and Departments of Physics, Computer Science and Biology, Northeastern University, Boston, Massachusetts 02115, USA.*

[6]*Center for Cancer Systems Biology, Dana-Farber Cancer Institute, Boston, Massachusetts 02115, USA.*

[7]*College of Computer and Information Science, Northeastern University, Boston, Massachusetts 02115, USA.*

*These authors contributed equally to this work.

Patient stratification or disease subtyping is crucial for precision medicine and personalized treatment of complex diseases. The increasing availability of high-throughput molecular data provides a great opportunity for patient stratification. In particular, many clustering methods have been employed to tackle this problem in a purely data-driven manner. Yet, existing methods leveraging high-throughput molecular data often suffers from various limitations, e.g., noise, data heterogeneity, high dimensionality or poor interpretability. Here we introduced an Entropy-based Consensus Clustering (ECC) method that overcomes those limitations all together. Our ECC method employs an entropy-based utility function to fuse many basic partitions to a consensus one that agrees

bioRxiv preprint doi: https://doi.org/10.1101/073189; this version posted September 3, 2016. The copyright holder for this preprint (which was not certified by peer review) is the author/funder. All rights reserved. No reuse allowed without permission.

with the basic ones as much as possible. Maximizing the utility function in ECC has a much more meaningful interpretation than any other consensus clustering methods. Moreover, we exactly map the complex utility maximization problem to the classic *K*-means clustering problem with a modified distance function, which can then be efficiently solved with linear time and space complexity. Our ECC method can also naturally integrate multiple molecular data types measured from the same set of subjects, and easily handle missing values without any imputation. We applied ECC to both synthetic and real data, including 35 cancer gene expression benchmark datasets and 13 cancer types with four molecular data types from The Cancer Genome Atlas. We found that ECC shows superior performance against existing clustering methods. Our results clearly demonstrate the power of ECC in clinically relevant patient stratification.

Introduction

High-throughput technologies, such as next-generation sequencing, have enabled us to rapidly accumulate a wealth of various molecular data types, including genome, transcriptome, proteome, and epigenome (*1*-*3*). Those massive genomics studies offer us great opportunities to characterize human pathologies and disease subtypes, identify driver genes and pathways, and nominate drug targets for precision medicine (*4, 5*). In particular, development of novel computational approaches for patient stratification leveraging high-throughput molecular data would significantly facilitate precision medicine and personalized treatment, which target

bioRxiv preprint doi: https://doi.org/10.1101/073189; this version posted September 3, 2016. The copyright holder for this preprint (which was not certified by peer review) is the author/funder. All rights reserved. No reuse allowed without permission.

discrete molecular subclasses of complex diseases with specific genetic or epigenetic profiles (*4*).

Clustering, an unsupervised exploratory analysis, has been widely used for patient stratification or disease subtyping (*6*). However, traditional clustering algorithms, such as *K*-means, hierarchical clustering, and spectral clustering, suffer from noise, data heterogeneity and high dimensionality that are associated with high-throughput molecular data (*7, 8*). *Ensemble clustering* (a.k.a. *consensus clustering*) can merge some individually generated basic partitions, and ensure the final consensus partition maximally agrees with the basic ones (*9*). This significantly helps us generate more robust clustering results, find bizarre clusters, better handle noise, outliers and sample variations, and integrate solutions from multiple distributed data sources (*9*). However, existing consensus clustering algorithms based on co-association matrix (*10*) are computationally expensive and require a large storage space, preventing them to handle high-throughput molecular data. Moreover, their interpretation of the consensus partition is often obscure.

Results

Methodology overview of ECC

Here we introduce a novel consensus clustering method, i.e. *Entropy-based Consensus Clustering* (ECC), for patient stratification. Consider an $n \times m$ matrix of molecular data of n subjects (or experiments, conditions, samples; corresponding to n rows) and m features (such as mRNAs; corresponding to m columns). Each subject can be represented by a point in the

bioRxiv preprint doi: https://doi.org/10.1101/073189; this version posted September 3, 2016. The copyright holder for this preprint (which was not certified by peer review) is the author/funder. All rights reserved. No reuse allowed without permission.

m -dimensional feature space, with different shapes representing different clusters the subjects belong to (**Fig. 1A**). There are three steps in the ECC pipeline. Step-1: We generate r basic partitions using K -means clustering with parameter K (i.e., the number of clusters) randomly chosen from 2 to $\sqrt{n}$ (see **Fig. 1B**) (*11*). Hereafter we call this kind of basic partitions generation strategy *Random Parameter Selection* (RPS). Note that in this step we can use any basic clustering method. Here we just choose K -means for its simplicity and high efficiency. In this work we choose $r = 100$ and find that larger r does not significantly improve the result. Step-2: We derive a binary matrix from each basic partition via 1-of-K coding, where K is the cluster number in this basic partition and only one element in each row is1, others are 0. We concatenate all those binary matrices into a large binary matrix (**Fig. 1C**). Step-3: We employ an entropy-based utility function to guide the fusion of all the r basic partitions into a consensus one (**Fig. 1D**). This is achieved by conducting K -means clustering on the binary matrix with a modified distance function and a user-defined cluster number K .

Our ECC method has three key features. First, it solves the consensus clustering problem in a *utility* way, which has more meaningful interpretation than any other consensus clustering methods. Here the utility function is applied to quantify the similarity between each of the r basic partitions and the consensus one. Maximizing the utility function requires us to find a single consensus partition that agrees with the basic ones as much as possible. Second, we uncover a remarkable equivalence relationship between an entropy-based utility function and a K -means distance function so that the complex utility maximization problem can be efficiently

bioRxiv preprint doi: https://doi.org/10.1101/073189; this version posted September 3, 2016. The copyright holder for this preprint (which was not certified by peer review) is the author/funder. All rights reserved. No reuse allowed without permission.

solved by the classic K-means method with a modified distance function (see **Supplementary Materials Sec. I.A)**. Consequently, both the time and space complexity of ECC are linear in n (see **Supplementary Materials Sec. I.B**). This dramatically improves the efficiency of ECC in real-world applications (*11*). Finally, ECC can naturally integrate multiple molecular data types measured from the same set of subjects, and easily handle missing values without any imputation (see **Materials and Methods**). This significantly increases the power of ECC in clinically relevant patient stratification.

To demonstrate that ECC indeed outperforms existing clustering methods, we compared the performance of ECC with five traditional clustering methods: Agglomerative Hierarchical Clustering with Average Linkage (AL), Single-Linkage (SL) and Complete-Linkage (CL), K-means Clustering (KM), and Spectral Clustering (SC); and two state-of-the-art consensus clustering methods: the Link-based Cluster Ensemble (LCE) and Approximate SimRank-based (ASRS) methods (*12*).

Evaluation using synthetic data

We first applied all those clustering methods to synthetic gene expression datasets with built-in cluster structure generated through a well-established dynamical gene regulation model (see **Supplementary Materials Sec. II)** (*13*). For fair comparison, we used two external indices of clustering validity: R_n (Normalized Rand Index) and NMI (Normalized Mutual Information) to objectively evaluate the performance of different clustering methods (*14*). Both R_n and

bioRxiv preprint doi: https://doi.org/10.1101/073189; this version posted September 3, 2016. The copyright holder for this preprint (which was not certified by peer review) is the author/funder. All rights reserved. No reuse allowed without permission.

NMI are positive cluster validity indices that estimate the quality of clustering results with respect to the underlying cluster structure of the data (see **Materials and Methods**). We found that ECC generally outperforms other methods in terms of its robustness against noise (see **Supplementary Materials Sec. IV.A**).

Evaluation using benchmark cancer gene expression data

We thenevaluated ECC and other clustering methods on 35 widely usedbenchmark cancer gene expression datasets(*15*) (**Supplementary Materials Sec. III.A**). The detailed description of the 35 datasets was provided in **Supplementary Table S2**. **Fig. 2A** shows the clustering performance of different algorithms measured by *NMI* . We found that for most datasets, the three consensus clustering methods (LCE, ASRS, and ECC) are superior to the five traditional clustering methods. Moreover, our ECC method achieves promising results on several datasets by a large margin, such as dataset-5 (*Armstrong-2002-v2*), dataset-9 (*Yeoh-2001-v1*), dataset-10 (*Chowdary-2006*) and dataset-13 (*Golub-1999-v1*). Although LCE and ASRS yield reasonable performance on several datasets, they suffer from low robustness. For example, ASRS achieves 100% accuracy on dataset-23 (*Nutt-2003-v3*), but it yields even worse results than that of random assignment on dataset-9 (*Chen-2002*). We emphasize that, for unsupervised tasks, robustness is much more important than performance in practice when dealing with highly heterogeneous molecular data types (such as mRNA expression)(*16*). Different from LCE and ASRS, ECC fuses the basic partitions in a utility way, which ensures highly meaningful interpretations with

bioRxiv preprint doi: https://doi.org/10.1101/073189; this version posted September 3, 2016. The copyright holder for this preprint (which was not certified by peer review) is the author/funder. All rights reserved. No reuse allowed without permission.

high stability for the final consensus partition (**Supplementary Materials Sec. I**). To compare the overall performance of those clustering methods over the 35 benchmark datasets, we proposed an average performance score (see **Materials and Methods**) and found that ECC revealed significant advantages over all other methods in terms of average performance score.

We notice that there are four specific datasets (*Gordon-2002*, *Khan-2001*, *Ramaswamy-2001* and *Shipp-2002*) for which all clustering methods yield very poor performance, most likely due to the presence of irrelevant or noisy features. We pointed that this difficulty cannot be easily resolved by any existing clustering methods. Yet, it can be alleviated by a complementary basic partition generation strategy of RPS, i.e., the *Random Feature Selection* (RFS) strategy, within the framework of ECC. To achieve that, we generate different sub-datasets by randomly selecting certain percentage of features (e.g., mRNAs) and then apply traditional clustering (e.g., K -means) to those sub-datasets to obtain basic partitions. Indeed, we find that for these four datasets, the performance of RFS exceeds RPS with all sampling ratios. This indicates that RFS helps us avoid noisy and irrelevant mRNA expressions (see **Supplementary Materials Sec. IV** for details).

In addition, ECC has tremendous merits in terms of computational cost. **Fig. 2B** shows the execution time (in logarithmic scale) of the three consensus clustering methods (LCE, ASRS and ECC). The time complexity of ECC is $O(InKr)$, where I is the number of iterations, n is the number of subjects, K is the number of clusters and r is the number of basic partitions. The space complexity of ECC is $O(nr)$. For LCE and ASRS, the space complexities are both

bioRxiv preprint doi: https://doi.org/10.1101/073189; this version posted September 3, 2016. The copyright holder for this preprint (which was not certified by peer review) is the author/funder. All rights reserved. No reuse allowed without permission.

$O(n^2)$; and the time complexities are $O(n^2 \log n)$ and $O(n^3)$, respectively. Naturally, ECC is more suitable for high-throughput molecular data analysis (**Supplementary Materials Sec. IV**). For example, on dataset-34 (*Yeoh-2002-v1*), ECC is 115 times and 1,600 times faster than LCE and ASRS, respectively.

Translational applications of ECC

The availability of massive and various molecular data types generated from large-scale and well-characterized cohorts across multiple cancer types provides an unprecedented opportunity for patient stratification. Here we demonstrated the translational applications of ECC based on13 major cancer types from The Cancer Genome Atlas (TCGA) project with sufficient sample size and clinical profiles for four molecular data types: mRNA expression (RNA-seq V2), microRNA (miRNA) expression, protein expression, and somatic copy number alterations (SCNAs), as shown in **Supplementary Table S3**. For fair comparison, we collected the empirical number of clusters (subtypes) for the 13 TCGA cancer types from previous studies. Then we applied survival analysis to evaluate the performance of different clustering methods in terms of $-\log_{10}(P)$ with P the log-rank test P-value (**Supplementary Materials Sec. V** and **Supplementary Tables S7-10**).

For each molecular data type (Protein, miRNA, mRNA, and SCNA), we calculated the clustering performance of ECC against other clustering methods across the 13 TCGA cancer types. We found that ECC outperformed other methods (in terms of the number of significant

bioRxiv preprint doi: https://doi.org/10.1101/073189; this version posted September 3, 2016. The copyright holder for this preprint (which was not certified by peer review) is the author/funder. All rights reserved. No reuse allowed without permission.

survival analysis results across the 13 TCGA cancer types, as highlighted in dotted red rectangles in **Fig. 3A-D**) for any single molecular data type.

By integrating the 4 different molecular data types, ECC generated significant clusters (cancer subtypes) for all the 13 TCGA cancer types ($P < 0.05$, log-rank test, **Table. 1**). Note that traditional clustering methods and existing consensus clustering methods cannot easily integrate multiple molecular data types, due to the presence of missing values for certain molecular data type of certain subjects. Yet, ECC can naturally resolve this issue by utility fusion, where missing values in basic partition provide no utility for the final fusion (**Supplementary Fig. S9**). Moreover, by integrating multiple molecular data types, ECC is effectively more robust to noise present in the data (partially because it has more data types to generate basic partitions). For example, in the case of uterine corpus endometrial carcinoma (UCEC), using any of the 4 molecular data types, ECC cannot yield significant clusters (**Fig. 4A**). Yet, by integrating multiple molecular data types (pan-omics), ECC yielded 4 significant clusters (**Fig. 4B**) with distinct patient survival curves ($P = 0.0043$, **Fig. 4C**); while using any single molecular data type the clusters generated by ECC do not pass the significance test of survival analysis ($P > 0.05$, **Supplementary Tables S7-10**). In addition, subtypes identified by ECC via integrating 4 molecular data types were closely associated with the clinical subtypes on a histological basis in UCEC (**Fig. 4D**). For instance, subtype 2 with most aggressive uterine tumor shows poor survival than subtype 1 with the less aggressive uterine tumors. Similar trends are also observed in ovarian serous cystadenocarcinoma (OV, $P = 7.79 \times 10^{-4}$) and prostate adenocarcinoma

bioRxiv preprint doi: https://doi.org/10.1101/073189; this version posted September 3, 2016. The copyright holder for this preprint (which was not certified by peer review) is the author/funder. All rights reserved. No reuse allowed without permission.

(PRAD, $P = 5.27\times10^{-4}$) (see **Supplementary Table S11**). Since TCGA clinical information may not be complete or rigorously annotated, future efforts of assessing the clinical utility of different subtypes on additional patient cohorts with more carefully annotated clinical variables are needed.

Discussion

In sum, we show that ECC owns significant advantages in terms of cluster validity, execution time and space complexity, and robustness compared with other clustering methods in patient stratification. We demonstrate that ECC with RFS strategy can alleviate the detriment effect of irrelevant and noisy features. Moreover, ECC displays superior performance on the pan-omics data by integrating multiple molecular data types than that of single molecular data type. We anticipate that integrating more types of both molecular and clinical data, such as somatic mutations, DNA methylation, functional genomic data generated from CRISPR/Cas9 (*17*), proteogenomics (*18*), radiomics (*19*), and electronic medical records (*20*), will further improve patient stratification. Altogether, our ECC method paves the way to a much more refined representation and understanding of various molecular data types, facilitating the development of precision medicine.

bioRxiv preprint doi: https://doi.org/10.1101/073189; this version posted September 3, 2016. The copyright holder for this preprint (which was not certified by peer review) is the author/funder. All rights reserved. No reuse allowed without permission.

Methods:

Consensus clustering

Here we introduce the basic ideas of consensus clustering in the context of omics data (e.g., gene expression) analysis. Consensus clustering was originally developed for fusing several existing partitions into a robust one (*1*), and has recently been applied to gene expression data analysis (*2,3*). For example, the link-based cluster ensemble (LCE) method first summarizes several basic partitions into a co-association matrix (that measures how often two instances simultaneously occur in the same cluster); then modifies the zero entries in the co-association matrix with the distance derived from the original data; and finally conducts spectral clustering to obtain the consensus partition (*2*). As a variant of the LCE method, the Approximate SimRank-based(ASRS) method employs very similar idea with slightly different modification on the zero entries in the co-association matrix (*3*).

Different from the existing consensus clustering methods (LCE and ASRS), our ECC method employs an entropy-based utility function for the guidance of fusing all the basic partitions into a consensus one, which has a more meaningful interpretation than existing consensus clustering methods. Let X denote a gene expression dataset with n subjects and m genes. A partition of X into K crisp clusters is represented as a collection of K subsets of instances in $C = \{C_k \mid k = 1,...,K\}$, with $C_k \cap C_{k'} = \varnothing, \forall k \neq k'$, and $\cup_{k=1}^{K} C_k = \mathrm{X}$, or as a label vector $\pi = (L_\pi(x_1),...,L_\pi(x_n))^{\mathrm{T}}$ where L_π maps x_l to some label in $\{1,2,...,K\}$, $1 \le l \le n$. Suppose we have r basic partitions denoted as $\{\pi^{(1)},\pi^{(2)},...,\pi^{(r)}\}$ generated by some traditional

bioRxiv preprint doi: https://doi.org/10.1101/073189; this version posted September 3, 2016. The copyright holder for this preprint (which was not certified by peer review) is the author/funder. All rights reserved. No reuse allowed without permission.

clustering method (e.g., K-means) and there are K_v clusters in $\pi^{(v)}$, for $1 \le v \le r$. The goal of consensus clustering is to find a consensus partition π by solving the following optimization problem:

$$\max_{\pi} \sum_{v=1}^{r} U(\pi, \pi^{(v)}), \tag{1}$$

where U is a utility function measuring the similarity at the partition-level between each basic partition and the consensus one. In other words, we expect to find an optimal partition that agrees with the basic ones as much as possible. Different utility functions measure the similarity of two partitions in different aspects, rendering different objective functions for consensus clustering. In this work, an entropy-based utility function is employed for its fast convergence and high quality (*4*).

Entropy-based Utility Function

The core of ECC is to fuse these basic partitions into a consensus one based on an entropy-based utility function, which assures the consensus clustering algorithm to be highly efficient and robust. As formulated in Eq. (1), a utility function is defined on two partitions π and $\pi^{(v)}$ to measures their similarity at partition-level. We can employ the following contingency table to calculate the entropy-based utility function.

bioRxiv preprint doi: https://doi.org/10.1101/073189; this version posted September 3, 2016. The copyright holder for this preprint (which was not certified by peer review) is the author/funder. All rights reserved. No reuse allowed without permission.

π \ $\pi^{(v)}$	C'_1	C'_2	$\cdots$	C'_{K_v}	$\sum$
C_1	n_{11}	n_{12}	$\cdots$	n_{1K_v}	n_{1+}
C_2	n_{21}	n_{22}	$\cdots$	n_{2K_v}	n_{2+}
$\cdot$	$\cdot$	$\cdot$	$\cdots$	$\cdot$	$\cdot$
C_K	n_{K1}	n_{K2}	$\cdots$	n_{KK_v}	n_{K+}
$\sum$	n_{+1}	n_{+2}	$\cdots$	n_{+K_v}	n

Here we have two partition π and $\pi^{(v)}$, which contain K and K_v clusters, respectively. We assume π is the ground truth, and $\pi^{(v)}$ is the clustering result generated by a specific clustering algorithm. Let n_{ij} denote the number of objects shared by cluster C_i in π and cluster $C_j^{'}$ in $\pi^{(v)}$. Define $n_{i+} = \sum_{j=1}^{K_v} n_{ij}$, and $n_{+j} = \sum_{i=1}^{K} n_{ij}$, $1 \le i \le K$, $1 \le j \le K_v$.

Based on the contingency table, for π and $\pi^{(v)}$ we define two discrete distributions $P_i^{(v)} = (n_{i1}^{(v)} / n_{k+}, ..., n_{iKv}^{(v)} / n_{k+}), \forall i$, and $P^{(v)} = (n_{+1}^{(v)} / n, ..., n_{+j}^{(v)} / n, ..., n_{+Kv}^{(v)} / n)$. Then we have

Definition 1 (U_H)**.** An *entropy-based utility function* U_H is defined as

$$U_H(\pi, \pi^{(v)}) = -\sum_{i=1}^{K} \frac{n_{i+}}{n} H(P_i^{(v)}) + H(P^{(v)}), \tag{2}$$

where H denotes the Shannon entropy.

Since Shannon entropy is a concave function, according to the Jensen's inequality, we can prove that $-\sum_{k=1}^{K} \frac{n_{k+}}{n} H(P_k^{(v)}) \ge -H(\sum_{k=1}^{K} \frac{n_{k+}}{n} P_k^{(v)}) = -H(P^{(v)})$, rendering that $U_H \ge 0$. A larger U_H indicates the higher utility from the two partitions in greater similarity. Note that U_H is

bioRxiv preprint doi: https://doi.org/10.1101/073189; this version posted September 3, 2016. The copyright holder for this preprint (which was not certified by peer review) is the author/funder. All rights reserved. No reuse allowed without permission.

asymmetric, with $U_H(\pi,\pi^{(v)}) \neq U_H(\pi^{(v)},\pi)$, if $\pi \neq \pi^{(v)}$.

Entropy-based Consensus Clustering

Although it is crucial to design a utility function, how to optimize it in an efficient way is another challenge. Thanks to the general K-means based Consensus clustering (*4*), which has substantial advantage in terms of efficiency; we can transform the optimization problem in Eq. (1) into a modified K-means clustering problem as follows.

Let $\mathbf{B} = (b_1,...,b_n)^{\mathrm{T}}$ be a binary matrix derived from r basic partitions $\{\pi^{(1)},\pi^{(2)},...,\pi^{(r)}\}$, with

$$b_l = (b_l^{(1)},...,b_l^{(v)},...,b_l^{(r)}), 1 \le l \le n, \tag{3}$$

$$b_l^{(v)} = (b_{l,1}^{(v)},...,b_{l,j}^{(v)},...,b_{l,K_v}^{(v)}), \tag{4}$$

$$b_{l,j}^{(v)} = \begin{cases} 1, & L_{\pi^{(v)}}(l) = j \\ 0, & \text{otherwise} \end{cases}. \tag{5}$$

Apparently, **B** is a $n \times \sum_{i=1}^{r} K_i$ binary matrix, with $\left|b_l^{(i)}\right| = 1, \forall l, v.$ For the Entropy-based Consensus Clustering, a K-means clustering is directly conducted on **B** with the following modified distance function.

$$f(b_l, m_k) = \sum_{v=1}^{r} D(b_l^{(v)} \,||\, m_k^{(v)}), \tag{6}$$

where $m_k = \left\langle m_k^{(1)},...,m_k^{(v)},...,m_k^{(r)} \right\rangle$ with $m_k^v = \sum_{b_l \in C_k} b_l^{(v)} / \left|C_k\right|$, and $D(b_l^{(v)} \,||\, m_k^{(v)})$ is the KL-divergence from $b_l^{(v)}$ to $m_k^{(v)}$.

By this means, the complex consensus clustering can be exactly mapped into a classic K

bioRxiv preprint doi: https://doi.org/10.1101/073189; this version posted September 3, 2016. The copyright holder for this preprint (which was not certified by peer review) is the author/funder. All rights reserved. No reuse allowed without permission.

-means clustering with a modified distance function, which has roughly linear time complexity and its convergence can also be guaranteed as well. The exactness of the mapping can be rigorously proved (see **Supplementary Materials Sec. I.A** for details). This mapping makes ECC very practical for large-scale molecular data analysis. Indeed only r elements are non-zero entries in each row of **B**, which leads the time complexity from $O(IKn\sum_{v=1}^{r}K_v)$ to $O(IKnr)$, where I is the number of iterations.

Handling missing values

Missing values are quite common in practice due to data collection or device failure, especially for the pan-omics data of a large population (in computer science, this kind of data is called multi-view). Typically there are two ways to handle those missing values. One is to just remove the instances (i.e., subjects) that have missing values in any single molecular data type (or any single view). Apparently, this is of great waste because those instances (subjects) might have values for many other views (molecular data types). The other way is to replace these missing values by default or average values. This would harm the original data structure and degrade the clustering performance. We can naturally resolve this challenging issue within the framework of ECC. In particular, we consider that those missing values, which lead to missing labels in the basic partitions, do not provide any utility for the consensus fusion. If a basic partition has missing labels, we call it an *incomplete basic partition* (IBP). For IBP, we directly

bioRxiv preprint doi: https://doi.org/10.1101/073189; this version posted September 3, 2016. The copyright holder for this preprint (which was not certified by peer review) is the author/funder. All rights reserved. No reuse allowed without permission.

denote $b_{l,j}^{(v)}$ as an all-zero vector, which will not be involved in the distance calculation and centroid update. The following is the distance function for IBP:

$$f(b_l, m_k) = \sum_{v=1}^{r} I(b_l^{(v)} \in \pi^{(v)}) D(b_l^{(v)} \,||\, m_k^{(v)}), \tag{7}$$

and $m_k = \left\langle m_k^{(1)}, ..., m_k^{(v)}, ..., m_k^{(r)} \right\rangle$ with

$$m_k^v = \frac{\sum_{b_l \in C_k \cap \pi^{(v)}} b_l^{(v)}}{\left| C_k \cap \pi^{(v)} \right|}. \tag{8}$$

Datasets

In this work, we use 110 synthetic datasets to systematically evaluate the performance of ECC. The 110 synthetic datasets are generated by a well-established dynamical gene regulation model (*5*):

$$\begin{aligned} \frac{dx_i}{dt} &= m_i \cdot f_i(y) - \lambda_i^{\text{mRNA}} \cdot x_i \\ \frac{dy_i}{dt} &= r_i \cdot x_i - \lambda_i^{\text{Prot}} \cdot y_i \end{aligned}, \tag{9}$$

where m_i is the maximum transcription rate, r_i is the translation rate, λ_i^{mRNA} and λ_i^{Prot} are the mRNA and protein degradation rates, and **x** and **y** are vectors of mRNA and protein concentration levels, respectively. $f_i(\cdot)$ computes the relative activation of gene. The topology of the gene regulatory network is encoded in the activation functions.

Among the 110 synthetic datasets, 55 of them are based on an Erdős–Rényi random network with 500 nodes (genes), and the other 55 are based on a human transcriptional regulation

bioRxiv preprint doi: https://doi.org/10.1101/073189; this version posted September 3, 2016. The copyright holder for this preprint (which was not certified by peer review) is the author/funder. All rights reserved. No reuse allowed without permission.

network of 2723 genes (*6*). Each dataset contains 200 subjects with its benchmark of 4 clusters (50 subjects in a cluster). Each dataset contains 200 subjects divided evenly into 4 groups (clusters). Each group has a specific set of knocked-out genes. A more detailed description of the synthetic datasets can be found in **Supplementary Materials Sec. I**.

Besides the 110 synthetic datasets, 35 widely used cancer gene expression benchmark datasets (*7*) are employed to test the cluster validity of ECC. Also, 13 cancer types with four molecular data types from TCGA with survival information are used for practical evaluation of ECC (**Supplementary Table S3**).

Evaluation metrics

Since the true labels for synthetic and benchmark datasets are available, we can apply external measurements to objectively evaluate the performance of different clustering algorithms. Although there are many external measurements, some of them are biased. According to Wu *et. al.* (*12*), two normalized external measurements, NMI and R_n are unbiased and hence can be chosen for proper evaluation of clustering performance. Both can easily be calculated from the contingency table.

Normalized Mutual Information (NMI) measures the mutual information between resulted cluster labels and ground truth labels, followed by a normalization operation to assure NMI ranges from 0 to 1. Mathematically, it is defined as:

bioRxiv preprint doi: https://doi.org/10.1101/073189; this version posted September 3, 2016. The copyright holder for this preprint (which was not certified by peer review) is the author/funder. All rights reserved. No reuse allowed without permission.

$$NMI = \frac{\sum_{i,j} n_{ij} \log \frac{n \cdot n_{ij}}{n_{i+} \cdot n_{+j}}}{\sqrt{\left(\sum_i n_{i+} \log \frac{n_{i+}}{n}\right)\left(\sum_j n_{j+} \log \frac{n_{+j}}{n}\right)}} \quad . \tag{10}$$

Normalized Rand Index, denoted as R_n measures the similarity between two partitions in a statistical way, which is defined as:

$$R_{\mathrm{n}} = \frac{\sum_{i,j}\binom{n_{ij}}{2} - \sum_i \binom{n_{i+}}{2} \cdot \sum_j \binom{n_{+j}}{2} \Big/ \binom{n}{2}}{\sum_i \binom{n_{i+}}{2}/2 + \sum_j \binom{n_{+j}}{2}/2 - \sum_i \binom{n_{i+}}{2} \cdot \sum_j \binom{n_{+j}}{2} \Big/ \binom{n}{2}} . \tag{11}$$

Note that both NMI and R_n are positive measurements, i.e. a better partition has a larger NMI or R_n value. Although R_n is normalized, it can still be negative, which means that the partition is even worse than random label assignment.

To compare the overall performance of those clustering algorithms over the 35 benchmark cancer expression datasets, we propose an average performance score as follows:

$$Avg(A_i) = \frac{1}{d} \sum_{j=1}^{d} \frac{V(D_j, A_i)}{\max_i V(D_j, A_i)}, \tag{12}$$

where $V(D_j, A_i)$ denotes the performance (i.e., R_n or NMI) of Algorithm A_i on dataset D_j and d is the total number of benchmark datasets.

Code availability

The MATLAB code is freely available at http://scholar.harvard.edu/yyl/ecc.

bioRxiv preprint doi: https://doi.org/10.1101/073189; this version posted September 3, 2016. The copyright holder for this preprint (which was not certified by peer review) is the author/funder. All rights reserved. No reuse allowed without permission.

References:

1. Uhlen, M. *et al.Mol. Syst. Biol.*12, 862 (2016).
2. Zhu, Q. *et al.Nat. Methods*12, 211-214 (2015).
3. Gentles, A.J. *et al.Nat. Med.*21, 938-945 (2015).
4. Friedman, A.A., Letai, A., Fisher, D.E. & Flaherty, K.T. *Nat. Rev. Cancer*15, 747-756 (2015).
5. Biankin, A.V., Piantadosi, S. & Hollingsworth, S.J. *Nature*526, 361-370 (2015).
6. Chang, H.Y. *et al.Proc. Natl. Acad. Sci. USA*102, 3738-3743 (2005).
7. Andor, N. *et al.Nat. Med.*22, 105-113 (2016).
8. Arnedos, M. *et al.Nat. Rev. Clin. Oncol.*12, 693-704 (2015).
9. Fred, A. & Ghosh, J. *J. Mach. Learn. Res.*3, 587-617 (2002).
10. Fred, A.L.N. & Jain, A.K. *IEEE Trans. Pattern Anal. Mach. Intell.*27, 835-850 (2005).
11. Wu, J.J., Liu, H.F., Xiong, H., Cao, J. & Chen, J. *IEEE Trans. Knowledge Data Engin.*27, 155-169 (2015).
12. Galdi, P., Napolitano, F. & Tagliaferri, R. *Comput. Intell. Methods Bioinformat. Biostatist.*8623, 57-67 (2015).
13. Schaffter, T., Marbach, D. & Floreano, D. *Bioinformatics*27, 2263-2270 (2011).
14. Wu, J.J., Xiong, H. & Chen, J. *KDD-09: 15th ACM SIGKDD Conf. Knowledge Discov. Data Mining* 877-885 (2009).
15. de Souto, M.C., Costa, I.G., de Araujo, D.S., Ludermir, T.B. & Schliep, A. *BMC*

bioRxiv preprint doi: https://doi.org/10.1101/073189; this version posted September 3, 2016. The copyright holder for this preprint (which was not certified by peer review) is the author/funder. All rights reserved. No reuse allowed without permission.

*Bioinformatics*9, 497 (2008).

16. Jain, A.K. *Pattern Recogn.Lett.*31, 651-666 (2010).

17. Sanchez-Rivera, F.J. & Jacks, T. *Nat. Rev. Cancer*15, 387-395 (2015).

18. Zhang, B. *et al.Nature*513, 382-387 (2014).

19. Aerts, H.J. *et al.Nat. Commun.*5, 4006 (2014).

20. Denny, J.C. *et al.Nat. Biotechnol.*31, 1102-1110 (2013).

21. Strehl, A. & Ghosh, J. Cluster ensembles—a knowledge reuse framework for combining multiple partitions. *Journal of Machine Learning Research* 3, 587–617 (2003).

22. Iam-on, N., Boongoen, T. & Garrett, S. Lce: a link-based cluster ensemble method for improved gene expression data analysis. *Bioinformatics* 26, 1513–1519 (2010).

23. Galdi, P., Francesco, N. & Roberto, T. Consensus clustering in gene expression. *Computational Intelligence Methods for Bioinformatics and Biostatistics* 57–67 (2014).

24. Wu, J., Liu, H., Xiong, H., Cao, J. & Chen, J. K-means-based consensus clustering: A unifiedview. *IEEE Transaction on Knowledge and Data Engineering* 27, 155–169 (2015).

25. Schaffter, T., Marbach, D. & Floreano, D. Genenetweaver: in silico benchmark generation and performance profiling of network inference methods. *Bioinformatics* 27, 2263–2270 (2011).

26. Han, H. *et al.* Trrust: a reference database of human transcriptional regulatory interactions. *Scientific reports* 5 (2015).

27. Souto, M., Costa, I., de Araujo, D., Ludermir, T. & Schliep, A. Clustering cancer gene

bioRxiv preprint doi: https://doi.org/10.1101/073189; this version posted September 3, 2016. The copyright holder for this preprint (which was not certified by peer review) is the author/funder. All rights reserved. No reuse allowed without permission.

expression data: a comparative study. *BMC bioinformatics* 9, 1–14 (2008).

28. Jain, A. Data clustering: 50 years beyond k-means. *Pattern recognition letters* 31, 651–666(2010).

29. Galdi, P., Napolitano, F. & Tagliaferri, R. Consensus clustering in gene expression. In *Proceedings of Computational Intelligence Methods for Bioinformatics and Biostatistics* (2014).

30. Cheung, Y. & Jia, H. Categorical-and-numerical-attribute data clustering based on a unified similarity metric without knowing cluster number. *Pattern Recognition* 46, 2228–2238 (2013).

31. Borjigin, S. & Guo, C. Non-unique cluster numbers determination methods based on stability in spectral clustering. *Knowledge and Information Systems* 36, 439–458 (2013).

32. Wu, J., Xiong, H. & Chen, J. Adapting the right measures for k-means clustering. In *Proceedings of ACM SIGKDD International Conference on Knowledge Discovery and Data Mining*(2009).

33. Zelnik-Manor, L. & Perona, P. Self-tuning spectral clustering. In *Proceedings of Advances in neural information processing systems* (2004).

Acknowledgments. We thank Rulla Tamimi and Edwin Silverman for valuable discussions. This work is supported in part by the John Templeton Foundation (Award number 51977), the National Academy of Sciences- Grainger Foundation Frontiers of Engineering Award (2000006959), NSF CNS Award (1314484), ONR award

bioRxiv preprint doi: https://doi.org/10.1101/073189; this version posted September 3, 2016. The copyright holder for this preprint (which was not certified by peer review) is the author/funder. All rights reserved. No reuse allowed without permission.

(N00014-12-1-1028), ONR Young Investigator Award (N00014-14-1-0484), and U.S. Army Research Office Young Investigator Award (W911NF-14-1-0218).

Contributions. Y.-Y.L. and Y.F. conceived the project. Y.-Y.L. designed the research. H.L. developed the code to perform ECC clustering and conducted all the cluster analyses. H.F. and R.Z developed the code to generate synthetic gene expression data. R.Z. collected cancer gene expression benchmark datasets. F.C. collected TCGA datasets and interpreted results. All authors analyzed the results. F.C., H.L., R.Z. and Y.-Y.L. wrote the manuscript. H.F. edited the manuscript.

Author Information The authors declare no competing financial interests. Correspondence and requests for materials should be addressed to F.Y. (yunfu@ece.neu.edu) or Y.-Y.L. (yyl @channing.harvard.edu).

bioRxiv preprint doi: https://doi.org/10.1101/073189; this version posted September 3, 2016. The copyright holder for this preprint (which was not certified by peer review) is the author/funder. All rights reserved. No reuse allowed without permission.

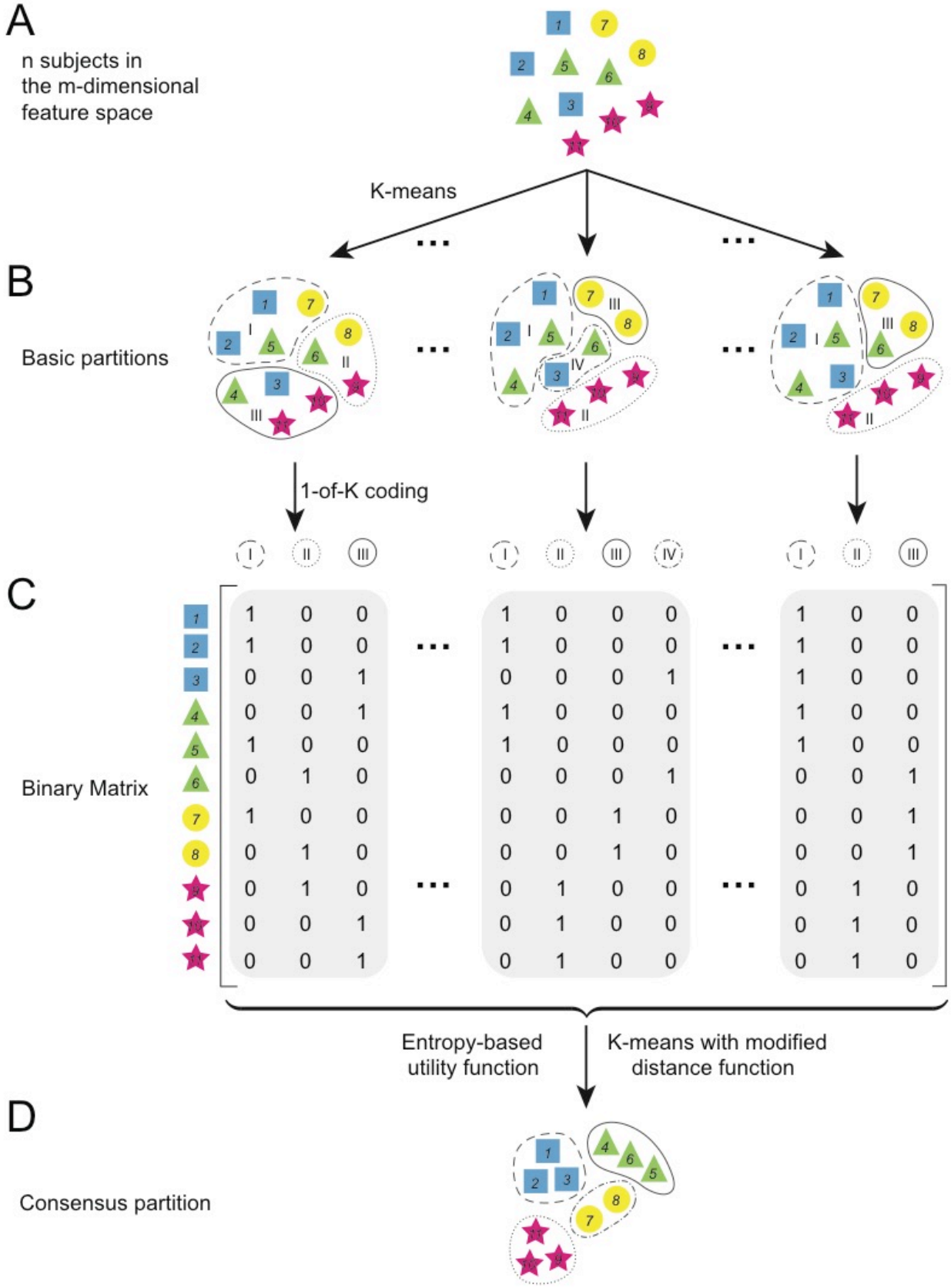

bioRxiv preprint doi: https://doi.org/10.1101/073189; this version posted September 3, 2016. The copyright holder for this preprint (which was not certified by peer review) is the author/funder. All rights reserved. No reuse allowed without permission.

Fig. 1. Schematic diagram of the ECC pipeline. (**A**) n subjects are presented by n points in the m-dimensional feature space. In this example, $n = 11$. The feature can be mRNA expression, Protein expression, or any other molecular data. Different shapes represent the subjects in different disease subtype (clusters). (**B**) K-means clustering is applied to the molecular data of the n subjects to obtain r basic partitions. For each basic partition, the cluster number K is randomly chosen from 2 to $\sqrt{n}$, and we highlight the K clusters using dashed line, dotted line, solid line, etc. (**C**) Each basic partition is transformed into 1-of-K coding, where K is the cluster number in each basic partition and only one element in each row is 1, others are 0. Concatenating all the basic partitions in 1-of-K coding form yields a large binary matrix $\mathbf{B}$, which is a new representation of the original molecular data. (**D**) A K-means clustering with modified distance function (derived from an entropy-based utility function) is conducted on the binary matrix $\mathbf{B}$ for the final consensus clustering. In this step, for synthetic and benchmark cancer gene expression datasets we set K to be the true cluster number. For the 13 TCGA cancer datasets, to fairly compare the ECC method and other clustering methods, we use the empirical number of clusters (subtypes) obtained from previous studies. For general molecular data when the empirical number of clusters is unknown, we can employ the cluster number estimation method in (*33*) to determine K for the final step of ECC.

bioRxiv preprint doi: https://doi.org/10.1101/073189; this version posted September 3, 2016. The copyright holder for this preprint (which was not certified by peer review) is the author/funder. All rights reserved. No reuse allowed without permission.

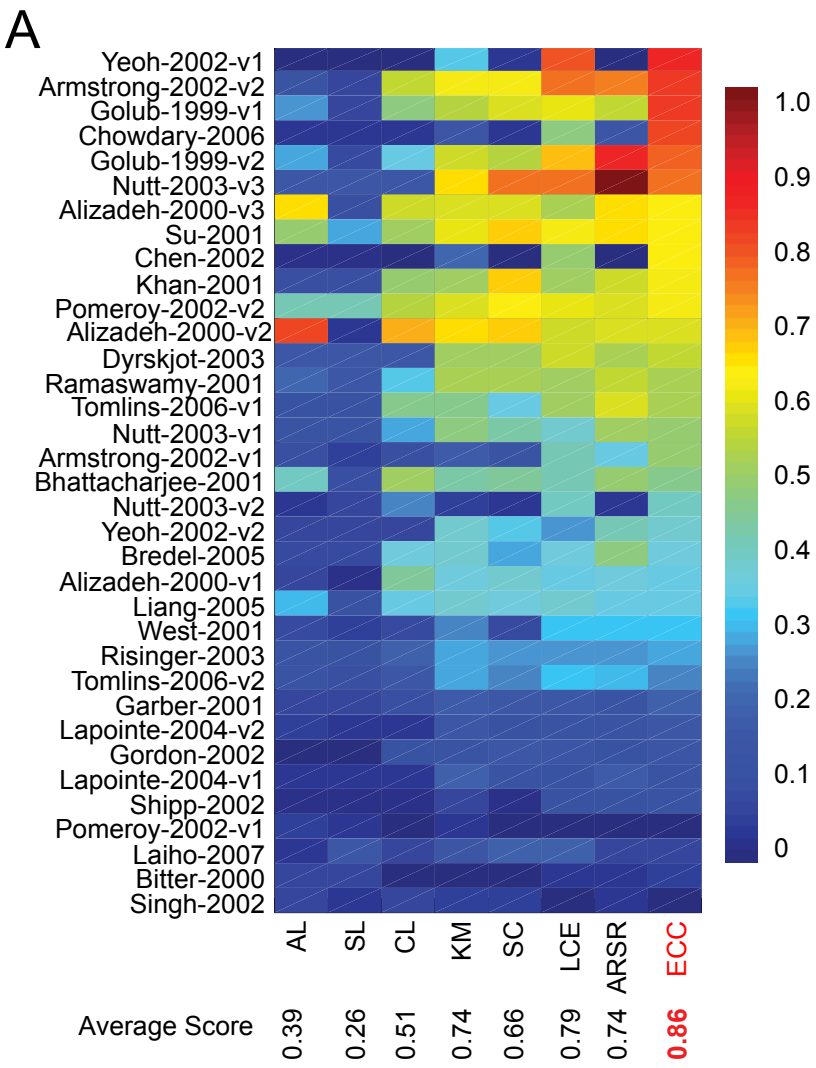

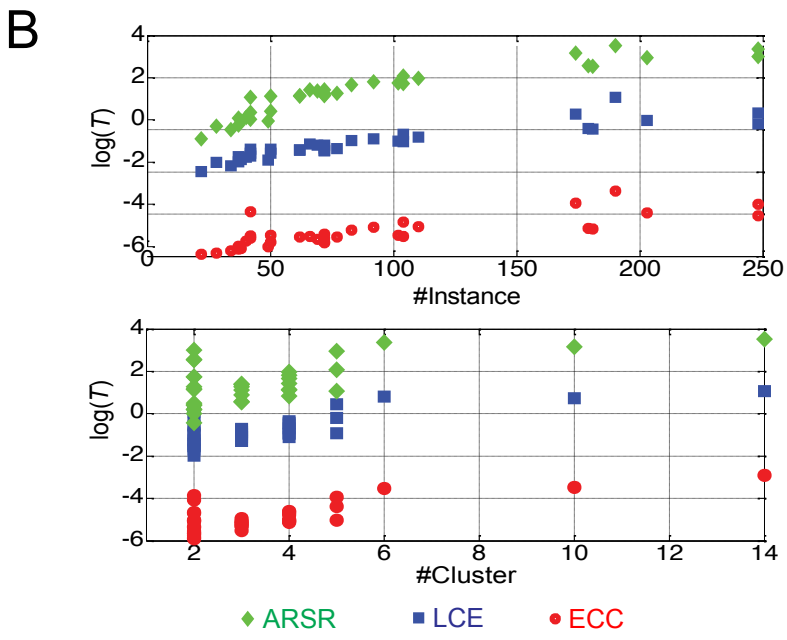

bioRxiv preprint doi: https://doi.org/10.1101/073189; this version posted September 3, 2016. The copyright holder for this preprint (which was not certified by peer review) is the author/funder. All rights reserved. No reuse allowed without permission.

Fig. 2. The performance of ECC on 35 benchmark cancer gene expression datasets. (**A**), The performance of different clustering methods (five traditional clustering methods: Agglomerative Hierarchical Clustering with Average Linkage (AL), Single-Linkage (SL) and Complete-Linkage (CL), K-means Clustering (KM), and Spectral Clustering (SC); and two state-of-the-art consensus clustering methods: the Link-based Cluster Ensemble (LCE) and Approximate SimRank-based (ASRS) methods) is measured by the Normalized Mutual Information (NMI). Overall, ECC outperforms the traditional clustering methods and state-of-the-art consensus clustering methods by a large margin. **(B)**, The execution time T (in logarithmic scale) of different consensus clustering methods (ARSR, LCE, and ECC) as a function of the number of instances or the number of classes.

bioRxiv preprint doi: https://doi.org/10.1101/073189; this version posted September 3, 2016. The copyright holder for this preprint (which was not certified by peer review) is the author/funder. All rights reserved. No reuse allowed without permission.

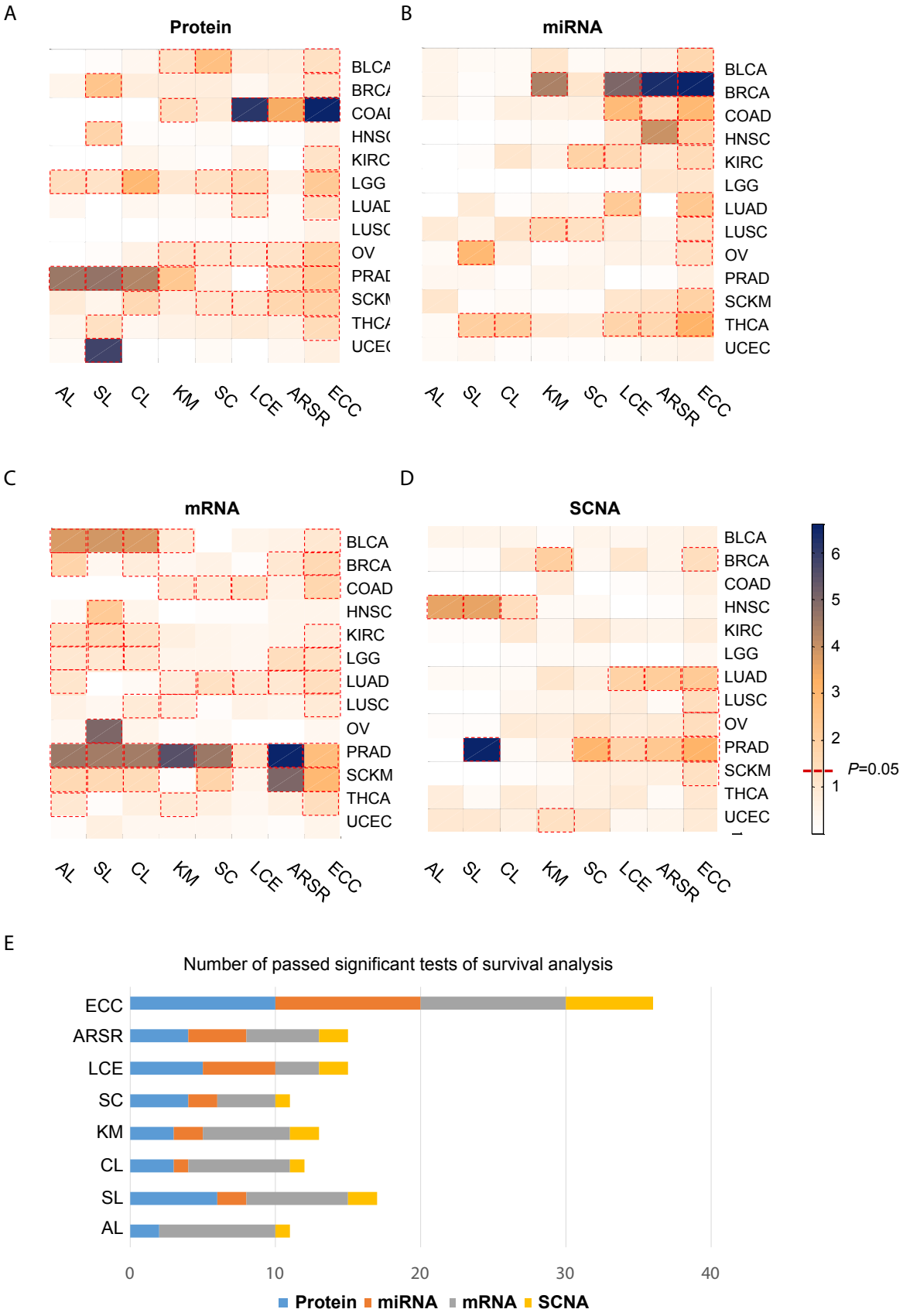

bioRxiv preprint doi: https://doi.org/10.1101/073189; this version posted September 3, 2016. The copyright holder for this preprint (which was not certified by peer review) is the author/funder. All rights reserved. No reuse allowed without permission.

Fig. 3. Performance of 7 different clustering methods on 4 molecular data types across 13 major cancer types from TCGA. Heatmaps show the survival analysis for 13 major cancer types using 7 different clustering methods based on four molecular data types: (**A**) protein expression (protein), (**B**) miRNA expression (miRNA), (**C**) mRNA expression (mRNA), and (**D**) somatic copy number alterations (SCNA), respectively. We use the $-\log(P)$ to draw the heatmap and elements with dotted red rectangles have $P<0.05$. (**E**), This plot displays for each clustering method the times that it passes the significant tests of survival analysis, i.e. the number of dotted red rectangles in (**A-D**), over the 13 cancer types and the 4 different molecular data types.

bioRxiv preprint doi: https://doi.org/10.1101/073189; this version posted September 3, 2016. The copyright holder for this preprint (which was not certified by peer review) is the author/funder. All rights reserved. No reuse allowed without permission.

ECC	Protein	miRNA	mRNA	SCNA	Integration
BLCA	0.0212	0.0124	0.0187	0.1910	0.0027
BRCA	0.0313	6.37E-08	0.0011	0.0375	0.0131
COAD	3.32E-09	5.91E-04	7.77E-04	0.2340	8.69E-06
HNSC	0.1820	0.0090	0.1160	0.3800	0.0323
KIRC	0.0313	0.0223	0.0314	0.1730	9.78E-04
LGG	0.0016	0.0751	0.0039	0.4130	0.0119
LUAD	0.0245	0.0028	0.0028	0.0067	2.87E-05
LUSC	0.1980	0.0442	0.0258	0.0425	0.0393
OV	0.0021	0.0375	0.2210	0.0359	7.97E-04
PRAD	0.0020	0.1840	8.59E-06	7.28E-04	5.72E-04
SKCM	0.0035	0.0076	3.94E-06	0.0491	0.0131
THCA	0.0138	3.75E-04	0.0024	0.1080	0.0035
UCEC	0.1310	0.2680	0.1240	0.1260	0.0043

Table. 1. Performance of ECC on 4 molecular data types and its integration across 13 major cancer types from TCGA. The performance is quantified by the log-rank test P-value of the survival analysis over the identified clusters (cancer subtypes). We highlight $P<0.05$ in red. With the integration of the 4 molecular data types, i.e., the pan-omics, ECC yields clusters that pass the significant test for all the 13 cancer types.

bioRxiv preprint doi: https://doi.org/10.1101/073189; this version posted September 3, 2016. The copyright holder for this preprint (which was not certified by peer review) is the author/funder. All rights reserved. No reuse allowed without permission.

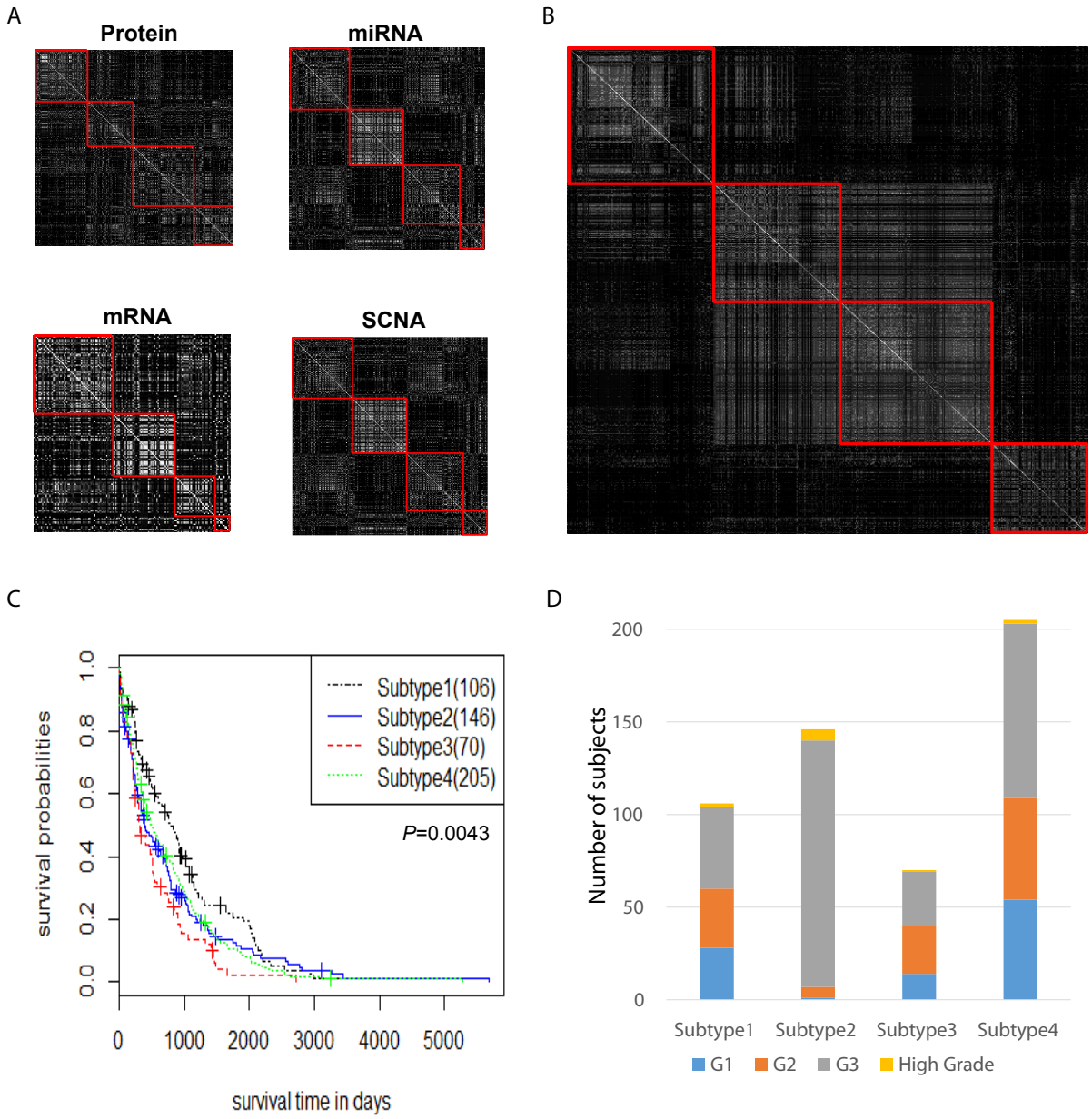

Fig. 4. Performance of ECC foruterine corpus endometrial carcinoma (UCEC) subjects from TCGA. The similarity matrices calculated from the 4 clusters generated by ECC using single molecular data type (**A**) and pan-omics data (**B**) of UCEC. The survival curves (**C**) and the composition of different clinical subtypes (**D**) for the 4 clusters generated by ECC using pan-omics data of UCEC.

bioRxiv preprint doi: https://doi.org/10.1101/073189; this version posted September 3, 2016. The copyright holder for this preprint (which was not certified by peer review) is the author/funder. All rights reserved. No reuse allowed without permission.

A Novel Clustering Algorithm for Patient Stratification
Supplementary Information

Hongfu Liu,* Rui Zhao,* Hongsheng Fang, Feixiong Cheng, Yun Fu,† and Yang-Yu Liu‡

(Dated: August 22, 2016)

* These two authors contributed equally.

† yunfu@ece.neu.edu

‡ yyl@channing.harvard.edu

bioRxiv preprint doi: https://doi.org/10.1101/073189; this version posted September 3, 2016. The copyright holder for this preprint (which was not certified by peer review) is the author/funder. All rights reserved. No reuse allowed without permission.

CONTENTS

I. Theoretical Analysis of ECC 3
A. Correctness of ECC 3
B. ECC Algorithm 5
C. Convergence of ECC 6

II. Synthetic Datasets 7
A. Dynamical Gene Regulation Model 7
B. Noise 8
1. Molecular Noise 8
2. Measurement Noise 9
C. Synthetic Disease Subtypes 10

III. Real-world Datasets 11
A. Benchmark Gene Expression Datasets 11
B. Molecular data from TCGA 11

IV. Additional Numerical Results 12
A. Performance of different clustering algorithms on synthetic data 12
B. Performance of different clustering algorithms on benchmark data sets 12
C. Impact of the basic partition number 12
D. Comparison of different basic partition generation strategies 12
E. Performance with missing values 13

V. Survival analysis 13
A. Log-rank test 14
B. Survival analysis on real-world data 14

References 15

bioRxiv preprint doi: https://doi.org/10.1101/073189; this version posted September 3, 2016. The copyright holder for this preprint (which was not certified by peer review) is the author/funder. All rights reserved. No reuse allowed without permission.

This file is the supplementary information for our paper "A Novel Clustering Algorithm for Patient Stratification", which contains the theoretical analysis of our ECC method, the generation of synthetic datasets, the description of real datasets, and additional numerical results.

I. THEORETICAL ANALYSIS OF ECC

In this work, we map the complicated utility optimization problem in ECC to a classic K-means clustering problem with a modified distance. Here we rigorously prove the correctness and convergence of ECC. We summarize all the variables used in this section in Table SI.

A. Correctness of ECC

To prove the correctness of ECC, we consider the following contingency matrix.

		$\pi^{(v)}$				
		C'_1	C'_2	$\cdots$	C'_{K_v}	$\sum$
π	C_1	n_{11}	n_{12}	$\cdots$	n_{1K_v}	n_{1+}
	C_2	n_{21}	n_{22}	$\cdots$	n_{2K_v}	n_{2+}
	$\cdot$	$\cdot$	$\cdot$	$\cdots$	$\cdot$	$\cdot$
	C_K	n_{K1}	n_{K2}	$\cdots$	n_{KK_v}	n_{K+}
	$\sum$	n_{+1}	n_{+2}	$\cdots$	n_{+K_v}	n

Here we have two partition π and $\pi^{(v)}$. We assume π is the ground truth, and $\pi^{(v)}$ is the clustering result returned by a certain clustering algorithm. Let n_{ij} denote the number of data objects shared by both cluster C'_j in $\pi^{(v)}$ and cluster C_i in π, $n_{i+} = \sum_{j=1}^{K_v} n_{ij}$, and $n_{+j} = \sum_{i=1}^{K} n_{ij}$, $1 \le i \le K, 1 \le j \le K_v$.

Let $\mathbf{B} = (b_1, \cdots, b_n)^\top$ be a binary matrix derived from r basic partitions $\pi^{(1)}, \cdots, \pi^{(r)}$, with

$$b_l = (b_l^{(1)}, \cdots, b_l^{(v)}, \cdots, b_l^{(r)}), 1 \le l \le n, \tag{S1}$$

$$b_l^{(v)} = (b_{l,1}^{(v)}, \cdots, b_{l,j}^{(v)}, \cdots, b_{l,K_v}^{(v)}), \tag{S2}$$

$$b_{l,j}^{(v)} = \begin{cases} 1, & \text{if } L_{\pi^{(v)}}(l) = j \\ 0, & \text{otherwise} \end{cases}. \tag{S3}$$

Apparently, $\mathbf{B}$ is a $n \times \sum_{i=1}^{r} K_i$ binary matrix, with $|b_l^{(i)}| = 1, \ \forall \ l, v$. For the Entropy-based Consensus Clustering, a K-means clustering is directly conducted on $\mathbf{B}$ with the modified distance function defined as follows.

bioRxiv preprint doi: https://doi.org/10.1101/073189; this version posted September 3, 2016. The copyright holder for this preprint (which was not certified by peer review) is the author/funder. All rights reserved. No reuse allowed without permission.

Theorem 1. *Assume π is a consensus partitioning of $\mathcal{X}$, with K clusters $C_1, \cdots, C_K$. Given r basic partitions $\pi_1, \cdots, \pi_r$, we have*

$$\max_{\pi} \sum_{v=1}^{r} U_H(\pi, \pi^{(v)}) \Leftrightarrow \min_{\pi} \sum_{k=1}^{K} \sum_{b_l \in C_k} \sum_{v=1}^{r} D(b_l^{(v)} \| m_k^{(v)}), \tag{S4}$$

where $m_k = (m_k^{(1)}, \cdots, m_k^{(v)}, \cdots, m_k^{(r)})$ with $m_k^{(v)} = \sum_{b_l \in C_k} b_l^{(v)}/|C_k|$, $D(b_l^{(v)}||m_k^{(v)})$ is the KL-divergence from $b_l^{(v)}$ to $m_k^{(v)}$ and U_H is the entropy-based utility function, which can be calculated as follow,

$$U_H(\pi, \pi^{(v)}) = -\sum_{i=1}^{K} \frac{n_{i+}}{n} H(P_i^{(v)}) + H(P^{(v)}), \tag{S5}$$

where $P_i^{(v)} = (n_{i1}^{(v)}/n_{k+}, \cdots, n_{iKv}^{(v)}/n_{k+})$, $\forall\ i$, and $P^{(v)} = (n_{+1}^{(v)}/n, \cdots, n_{+j}^{(v)}/n, \cdots, n_{+Kv}^{(v)}/n)$.

Proof. According to Bregmen Divergence[3], we have that $D(x\|y) = \sum_i x_i \log \frac{x_i}{y_1} = -H(x) + H(y) + (x-y)^\top \nabla H(y)$, where $H(x) = -\sum_i x_i \log x_i$ is the Shannon entropy. Hence we have

$$\begin{aligned} &\underbrace{\sum_{k=1}^{K} \sum_{b_l \in C_k} \sum_{v=1}^{r} D(b_l^{(v)} \| m_k^{(v)})}_{(\alpha)} \\ &= \sum_{k=1}^{K} \sum_{b_l \in C_k} \sum_{v=1}^{r} (-H(b_l^{(v)}) + H(m_k^{(v)})) + \underbrace{\sum_{k=1}^{K} \sum_{b_l \in C_k} \sum_{v=1}^{r} (b_l^{(v)} - m_k^{(v)})^\top \nabla H(m_k^{(v)})}_{(\beta)}. \end{aligned} \tag{S6}$$

Since $m_k^{(v)} = \sum_{b_l \in C_k} b_l^{(v)}/|C_k|$, we have $\sum_{b_l \in C_k} (b_l^{(v)} - m_k^{(v)}) = 0$, which indicates that the term $(\beta) = 0$. We therefore have:

$$\begin{aligned} (\alpha) &= -\sum_{k=1}^{K} \sum_{b_l \in C_k} \sum_{v=1}^{r} H(b_l^{(v)}) + \sum_{k=1}^{K} \sum_{b_l \in C_k} \sum_{v=1}^{r} H(m_k^{(v)}) \\ &= \underbrace{-\sum_{v=1}^{r} \sum_{b_l \in \mathbf{B}} H(b_l^{(i)})}_{(\gamma)} + n \sum_{v=1}^{r} \sum_{k=1}^{K} p_{k+} H(m_k^{(v)}), \end{aligned} \tag{S7}$$

where $p_{k+} = n_{k+}/n$. Since the term (γ) and n are constants, we have

$$\min_{\pi}(\alpha) \Leftrightarrow \max_{\pi} \Big[-\sum_{i=1}^{r} \sum_{k=1}^{K} p_{k+} H(m_k^{(v)}) \Big]. \tag{S8}$$

Note that $m_{k,j}^{(v)} = \sum_{b_l \in C_k} b_{l,j}^{(v)}/|C_k| = |C_k \bigcap C_j^{(v)}|/|C_k| = n_{kj}^{(v)}/n_{k+}$, $\forall\ j$, which indicates that

$$m_k^{(v)} = \left(\frac{n_{ki}^{(v)}}{n_{k+}}, \cdots, \frac{n_{kK_i}^{(v)}}{n_{k+}} \right) = P_k^{(v)}, \forall\ k, i. \tag{S9}$$

bioRxiv preprint doi: https://doi.org/10.1101/073189; this version posted September 3, 2016. The copyright holder for this preprint (which was not certified by peer review) is the author/funder. All rights reserved. No reuse allowed without permission.

If we substitute $m_k^{(v)}$ by $P_k^{(v)}$ in Eq. S8, and add the constant $\sum_{v=1}^{r} H(P^{(v)})$ to the right-hand-side, we finally have

$$\begin{aligned}\sum_{k=1}^{K}\sum_{b_l\in C_k}\sum_{v=1}^{r} D(b_l^{(v)}\|m_k^{(v)}) &\Leftrightarrow \max_{\pi}\sum_{v=1}^{r}(-\sum_{k=1}^{K} p_{k+}H(P_k^{(v)}) + H(P^{(v)})) \\ &\Leftrightarrow \max_{\pi}\sum_{v=1}^{r} U_H(\pi,\pi^{(v)}),\end{aligned} \tag{S10}$$

and the theorem thus follows. □

Remark 1. *Theorem 1 gives a new insight of the objective function. ECC aims to find a partition that agrees with the basic ones as much as possible and employs U_H to measure the similarity of two partitions. Theorem 1 ensures that we can calculate the distance of two partitions by KL-divergence to achieve the same goal.*

Remark 2. *By Theorem 1, we can solve the consensus clustering problem by the classic K-means clustering, which is the fastest clustering algorithm. Recall that only r elements are non-zero entries in each row of $\boldsymbol{B}$, thus the positions for these non-zero elements are needed, rendering the time complexity $O(IKnr)$, where I is the iteration number. Usually, I, K, r are smaller than n. Therefore, the time complexity of ECC is roughly linear to the number of instances, which is suitable for high-throughput molecular data analysis.*

B. ECC Algorithm

The pseudo code of our ECC algorithm is shown in Algorithm 1. In essence, ECC is a variant of K-means, which has the two-phase iteration: instance assignment and centroid update. The only difference between ECC and K-means is the distance function. In K-means, the squared Euclidian distance is employed, while we use a summation of several KL-divergence in ECC.

ECC has tremendous merits in terms of efficiency over the other methods. Fig. S8 shows the execution time (in logarithmic scale) of three consensus clustering methods (LCE, ASRS and ECC). The time complexity of ECC is $\mathcal{O}(InKr)$, where I is the iteration number, n is the subject number, K is the class number and r is the number of basic partitions. The space complexity of ECC is $\mathcal{O}(nr)$. For LCE and ASRS, the space complexities are both $\mathcal{O}(n^2)$ and the time complexities are $\mathcal{O}(n^2 \log n)$ and $\mathcal{O}(n^3)$, respectively.

bioRxiv preprint doi: https://doi.org/10.1101/073189; this version posted September 3, 2016. The copyright holder for this preprint (which was not certified by peer review) is the author/funder. All rights reserved. No reuse allowed without permission.

Algorithm 1 The algorithm of Entropy-based Consensus Clustering

Input: $\mathcal{X}$: data matrix, $n \times m$;

K: number of clusters;

r: number of basic partitions.

Output: Partition π;

1: Obtain the set of basic partitions Π by some generation strategy;

2: Build the binary matrix B by Eq.(6-8) in the main paper;

3: Randomly select K instances from B as centroids;

4: **repeat**

5: Assign each instance to its closest centroid by the distance function in Eq.(9) in the main paper;

6: Update centroids by arithmetic mean;

7: **until** K centroids remain unchanged.

8: Return the partition π.

C. Convergence of ECC

ECC is solved by the K-means clustering with a modified distance function. The convergence of ECC is assured by the following theorem [4].

Theorem 2. *For the objective function in Theorem 1, ECC is guaranteed to converge in finite two-phase iterations of K-means clustering .*

Proof. The K-means distance function can be generalized as the Bregman divergences[3],

$$f(x, y) = \phi(x) - \phi(y) - (x - y)^\top \nabla\phi(y), \tag{S11}$$

where $\phi(\cdot)$ is a convex function. By using Bregman divergences, the convergence of K-means is guaranteed [3].

For the objective function in Theorem 1, we have

$$\phi(x) = \sum_{v=1}^{r} H(x^{(v)}), \tag{S12}$$

which is the summation of the Shannon Entropy. Since $H(\cdot)$ is a convex function and the summation preserves the convex property, therefore the distance function in Theorem 1 is a Bregman divergence, the convergence of ECC can then be guaranteed. □

In handling IBPs, the convergence property of ECC still holds.

bioRxiv preprint doi: https://doi.org/10.1101/073189; this version posted September 3, 2016. The copyright holder for this preprint (which was not certified by peer review) is the author/funder. All rights reserved. No reuse allowed without permission.

II. SYNTHETIC DATASETS

The 110 synthetic gene expression datasets are generated through a well-known dynamical gene regulation model[1]. To be self-contained, we summarize all the variables used in this section in Table SII.

A. Dynamical Gene Regulation Model

This model is based on a gene regulatory network represented by a digraph $G(V, E)$. Here V is the set of nodes (genes) and E is the set of directed edges (gene regulations). Both transcription and translation are modeled using a standard thermodynamic approach[1]. For each node v_i, i=1,2,...,n, the changing rate of mRNA concentration F_i^{mRNA} and the changing rate of protein concentration F_i^{Prot} are described by a set of coupled ordinary differential equations (ODEs):

$$F_i^{\mathrm{mRNA}}(\mathbf{x}, \mathbf{y}) = \frac{dx_i}{dt} = m_i \cdot f_i(\mathbf{y}) - \lambda_i^{\mathrm{mRNA}} \cdot x_i, \tag{S13a}$$

$$F_i^{\mathrm{Prot}}(\mathbf{x}, \mathbf{y}) = \frac{dy_i}{dt} = r_i \cdot x_i - \lambda_i^{\mathrm{Prot}} \cdot y_i, \tag{S13b}$$

where m_i is the maximum transcription rate, r_i is the translation rate, $\lambda_i^{\mathrm{mRNA}}$ and $\lambda_i^{\mathrm{Prot}}$ are the mRNA and protein degradation rates, $\mathbf{x} \in \mathbf{R}^n$ and $\mathbf{y} \in \mathbf{R}^n$ are vectors of mRNA and protein concentration levels, respectively. $f_i(\cdot)$ is the activation function of gene i , which is between 0 (gene i is turned off) and 1(gene i is maximally activated) given the protein concentrations $\mathbf{y}$. The network topology is encoded in the activation functions. A more detailed definition of $f_i(\cdot)$ is as follows.

We use a standard thermodynamics-based approach to model gene regulation[1]. The basic assumption is that binding of transcription factors (TFs) to cis-regulatory sites on the DNA is in quasiequilibrium because it is orders of magnitude faster than transcription and translation. In the simplest cases, gene i is regulated by a single TF (e.g. TF_j), then its promoter has only two states: either the TF_j is bound (state S_1) or un-bound (state S_0). The probability $P(S_1)$ that gene i is in state S_1 at a certain time instant is given by the fractional saturation:

$$P(S_1) = \frac{v_j}{1 + v_j}, \tag{S14}$$

$$v_j = (\frac{y_j}{k_{ij}})^{h_{ij}}, \tag{S15}$$

where y_j is the concentration of TF_j, k_{ij} is the dissociation constant, and h_{ij} the Hill coefficient. The bound TF activates or represses the expression of the gene. In state S_0, the relative activation

bioRxiv preprint doi: https://doi.org/10.1101/073189; this version posted September 3, 2016. The copyright holder for this preprint (which was not certified by peer review) is the author/funder. All rights reserved. No reuse allowed without permission.

is α_0; in state S_1, the relative activation is α_1. Given $P(S_1)$ and its complement $P(S_0) = 1 - P(S_1)$, we can derive the function $f_i(y_j)$, which computes the mean activation of the gene i as a function of the TF concentration y_j:

$$f_i(y_j) = \alpha_0 P(S_0) + \alpha_1 P(S_1) = \frac{\alpha_0 + \alpha_1 v_j}{1 + v_j}. \tag{S16}$$

We can also consider gene i has two regulatory inputs. The resulting expression would be:

$$f_i(y_j) = \frac{\alpha_0 + \alpha_1 v_j + \alpha_2 v_l + \alpha_3 \rho v_j v_l}{1 + v_j + v_l + \rho v_j v_l}, v_j = (\frac{y_j}{k_{ij}})^{h_{ij}}, v_l = (\frac{y_l}{k_{il}})^{h_{il}}, \tag{S17}$$

where ρ is the cooperativity factor, and α_i are the relative activations when none of the TFs (α_0), only the first (α_1), only the second (α_2) or both TFs are bound (α_3).

This approach can be used for an arbitrary number of regulatory inputs. If a gene is regulated by N TFs, it will have 2^N states: each of the TFs can be bound or un-bound. Thus, the function for N regulators would be:

$$f(\mathbf{y}) = \sum_{t=0}^{2^N - 1} \alpha_t P(S_t). \tag{S18}$$

Based on thermodynamics, we can compute the probability $P(S_t)$ for every state t.

Assume now we have the gene regulatory network $G(V, E)$ and the detailed dynamical model parameters. The initial values of x_i and y_i are generated randomly from the interval [0.001, 1]. Then we can compute the time evolution of $\mathbf{x}$ and $\mathbf{y}$ until the system reaches a steady state.

B. Noise

The integration of the coupled ODEs (Eq.S1a and Eq.S1b) results in noiseless mRNA and protein concentration levels. However, both molecular and measurement noise in gene expressions are unavoidable in practice. In living cells, molecular noise originates from thermal fluctuations and stochastic processes such as transcription and translation. Moreover, measurement noise of gene expression depends on the experimental technology used to monitor the gene expression level.

1. Molecular Noise

Both F_i^{mRNA} and F_i^{Prot} can be written as follows:

$$\frac{dX_t}{dt} = V(X_t) - D(X_t), \tag{S19}$$

bioRxiv preprint doi: https://doi.org/10.1101/073189; this version posted September 3, 2016. The copyright holder for this preprint (which was not certified by peer review) is the author/funder. All rights reserved. No reuse allowed without permission.

where $V(X_t)$ is the production term and $D(X_t)$ is the degradation term of mRNA or protein. To model molecular noise in the transcription and translation processes, we can use the following chemical Langevin equation (CLE):

$$\frac{dX_t}{dt} = V(X_t) - D(X_t) + c_1(\sqrt{V(X_t)}\eta_v + \sqrt{D(X_t)}\eta_d), \tag{S20}$$

where η_v and η_d are independent Gaussian white-noise processes, c_1 is a constant to integrate two equations to control the amplitude of the molecular noise.

To solve the CLE, we can use the Stratonovich scheme and the Milstein method. Stratonovich Scheme is a technique used in stochastic integral, which is very similar to *Ito* integral. Suppose we have a stochastic differentiable equation:

$$dX_t = f(X_t, t)dt + g(X_t, t)dW_t, \tag{S21}$$

where X_t is the random variable, f is the drift coefficient, g is the diffusion coefficient, and W_t is the Wiener Process. Integrating both sides yields:

$$X_t = X_{t_0} + \int_{t_0}^{t} f(X_s, s)ds + \int_{t_0}^{t} g(X_s, s) \circ dW_s, \tag{S22}$$

where $\circ$ is used here to distinguish Stratonovich from *Ito*.

We compute the integrals in Eq. S10 using the Milstein method. Milstein method has two versions, namely a normal one and a derivative-free version. For simplicity, we use derivative-free Milstein method:

$$X_{n+1} = X_n + f_n h + g_n \delta W_n + \frac{1}{2\sqrt{h}}[g(\overline{X_n}) - g_n](\delta W_n)^2, \tag{S23}$$

where

$$h = t_{n+1} - t_n, \tag{S24}$$

$$\overline{X_n} = X_n + f_n h + g_n \sqrt{h}, \tag{S25}$$

$$\delta W_n = [W_{t+h} - W_t] \sim \sqrt{h}\mathcal{N}(0, 1), \tag{S26}$$

Then we update X until it reaches a steady state.

2. Measurement Noise

The measurement noise depends on the technology used to monitor level of gene expression and hence is modeled independently of the molecular noise. In this work, we model the measurement

bioRxiv preprint doi: https://doi.org/10.1101/073189; this version posted September 3, 2016. The copyright holder for this preprint (which was not certified by peer review) is the author/funder. All rights reserved. No reuse allowed without permission.

noise as follows:

$$\tilde{X}_t = X_t + c_2 \cdot \eta_\omega, \tag{S27}$$

where X_t is computed from Eq.S1, η_ω represents independent Gaussian white-noise processes, and c_2 is a constant quantifying the measurement noise level.

C. Synthetic Disease Subtypes

In order to generate synthetic disease subtypes, we first generate a random digraph G to represent the gene regulatory network. Considering the exponential time complexity of calculating the activation function, we set the average in-degree $k_{\text{in}} = 2$ in the digraph G. Regarding the model parameters in Eq.S1, we choose m_i and r_i randomly from the interval [0, 1]. The Hill coefficient h_{ij} is sampled from a Gaussian distribution $\mathcal{N}(2, 4)$ bounded in the interval [1, 10]. An example of the gene regulatory network of 20 genes is shown in Fig. S1**a**. The time evolution of mRNA concentration levels $x_i(t)$ without noise, with only molecular noise, and with both molecular and measurement noise, are shown in Fig. S1**b**, Fig. S1**c**, Fig. S1**d**, respectively. This serves as the baseline model.

To simulate gene expression data for different disease subtypes, we assume that different disease subtypes are associated with different sets of genes that are knocked out. For those knock-out genes, we set their transcription rates m_i to be zero. Suppose in total we have N subjects divided into four groups (G_0, G_1, G_2, G_3) evenly: subjects in G_0 are generated from the baseline model, while subjects in G_1, G_2 and G_3 have different sets of knock-out genes (see Fig. S2). For each group (disease subtype), different subjects are simulated from different initial conditions of $\mathbf{x}$ and $\mathbf{y}$.

bioRxiv preprint doi: https://doi.org/10.1101/073189; this version posted September 3, 2016. The copyright holder for this preprint (which was not certified by peer review) is the author/funder. All rights reserved. No reuse allowed without permission.

III. REAL-WORLD DATASETS

We analysed 35 benchmark cancer gene expression datasets[2] with label (i.e. cluster structure) information to fully evaluate the performance of ECC, as well as 13 real cancer gene expression datasets with survival information available for practical evaluation. Some key characteristics of these datasets are summarized in Table SIII and Table SIV.

A. Benchmark Gene Expression Datasets

For the 35 benchmark datasets in Table SIII, the numbers of subjects vary from 22 to 248, the numbers of genes vary from 85 to 4,553 and the numbers of clusters vary from 2 to 14. Some datasets are from the same source. For example, dataset 2 and 3 (*Alizadeh-2000-v2, Alizadeh-2000-v3*) share the same gene expression data, but with different cluster numbers; dataset-4 and 5 (*Armstrong-2002-v1, Armstrong-2002-v2*) have the same subject number, but different dimensions of gene expression; dataset-14 (*Golub-1999-v2*) splits one cluster in dataset-15 (*Golub-1999-v1*) into two; dataset-32 (*Tomlins-2006-v2*) has one more cluster than the dataset-33 (*Tomlins-2006-v2*).

B. Molecular data from TCGA

Furthermore, we also analysed 13 molecular data from 13 major cancer types from The Cancer Genome Atlas (TGCA, https://tcga-data.nci.nih.gov/tcga/, date: 4/16/2016) project with survival information available. These cancer types include bladder urothelial carcinoma (BLCA), breast cancer carcinoma (BRCA), colon adenocarcinoma (COAD), head and neck squamous cell carcinoma (HNSC), kidney renal clear cell carcinoma (KIRC), acute myeloid leukemia (LAML), brain lower grade glioma (LGG), lung adenocarcinoma (LUAD), lung squamous cell carcinoma (LUSC), ovarian serous cystadenocarcinoma (OV), prostate adenocarcinoma (PRAD), skin cutaneous melanoma (SKCM), thyroid carcinoma (THCA), and uterine corpus endometrial carcinoma (UCEC). Each dataset contains 4 different types of molecular data, including protein expression, microRNA (miRNA) expression, mRNA expression (RNA-seq V2) and somatic copy number alterations (SCNAs). Note that the numbers of subjects varies in different data types.

bioRxiv preprint doi: https://doi.org/10.1101/073189; this version posted September 3, 2016. The copyright holder for this preprint (which was not certified by peer review) is the author/funder. All rights reserved. No reuse allowed without permission.

IV. ADDITIONAL NUMERICAL RESULTS

In this section, we provide more numerical results on ECC in terms of synthetic datasets evaluation, the number of basic partitions and the basic partition generation strategy.

A. Performance of different clustering algorithms on synthetic data

Figure S3 and S4 show the performance of different clustering algorithms on the 110 synthetic datasets with different settings. We find that for most datasets ECC achieves better performance than both traditional and previous ensemble clustering methods. For the four cases when ECC is not the best, the difference between the best one and ECC is within a small margin.

B. Performance of different clustering algorithms on benchmark data sets

Table S Vand SVI show the performance of different clustering algorithms in terms of R_n and NMI.

C. Impact of the basic partition number

To fully uncover the properties of ECC for practical use, we thoroughly explore some impact factors of ECC. Fig. S5 shows the performance of ECC as a function of the number r. Generally speaking, the performance goes up with larger r, and the variance becomes smaller. The number of basic partitions determines the stability of ECC. We find that $r = 100$ is large enough for a robust partition.

D. Comparison of different basic partition generation strategies

So far we employ Random Parameter Selection (RPS) strategy to generate basic partitions by K-means with different cluster numbers. A complementary strategy is the so-called Random Feature Selection (RFS) strategy. In RFS, we generate a subdata set by randomly selecting certain percentage of features (e.g. gene expressions), where K-means with a fixed cluster number is conducted to obtain the basic partitions. Fig. S6 demonstrates the performance of these two generation strategies. For these four datasets (15, 16, 26 and 28), RFS has better performance than RPS on all percentages of sampling ratio. For example, the improvements on dataset-15

bioRxiv preprint doi: https://doi.org/10.1101/073189; this version posted September 3, 2016. The copyright holder for this preprint (which was not certified by peer review) is the author/funder. All rights reserved. No reuse allowed without permission.

(*Gordon-2002*) are over 80% and 40% in terms of R_n and NMI. This indicates that only a subset of features (genes) reflect the true cluster structure, the rest are irrelevant or noisy. Finding discriminative features (genes) is a very challenging task, especially in unsupervised scenarios. Here we employ the simple RFS strategy and fuse these basic partitions to obtain promising results. Taking the efficiency into account, 10% sampling ratio is good enough for a satisfactory partition. Fig. S7 shows the comparison between the results derived from RPS and RFS (with 10% sampling ratio). We find that indeed RFS is a complementary basic partition generation strategy of RPS.

E. Performance with missing values

We validate the performance of ECC in the presence of missing values, which result in incomplete basic partitions (IBPs). Given a dataset, we randomly remove certain instances and call K-means clustering algorithm on the rest instances with the user-defined cluster number. For these removed instances, the labels are assigned to be 0 in the incomplete basic partitions. We repeat the above process 100 times to obtain 100 IBPs and employ ECC to get the consensus one. Fig. S9 shows the performance of ECC with different missing ratios on 4 datesets. We find that ECC can still provide high quality and robust consensus partition even with high missing ratio.

V. SURVIVAL ANALYSIS

For real-world molecular data without label information (e.g. the 13 TCGA cancer types analyzed in this work), we can employ survival analyses to evaluate the performance of different clustering methods. Survival analysis considers the expected duration of time until one or more events happen, such as death, disease occurrence, disease recurrence, recovery, or other experience of interest[5]. The duration of time measures the time from the beginning of an observation period (such as surgery or beginning treatment) to an event, or end of the study, or loss of contact or withdrawal from the study. Censoring/Censored observation means that, if a subject does not have an event during the observation time, they are described as censored. The subject is censored in the sense that nothing is observed or known about that subject after the time of censoring. A censored subject may or may not have an event after the end of observation time.

bioRxiv preprint doi: https://doi.org/10.1101/073189; this version posted September 3, 2016. The copyright holder for this preprint (which was not certified by peer review) is the author/funder. All rights reserved. No reuse allowed without permission.

A. Log-rank test

The log-rank test is a hypothesis test to compare the survival distributions of two or more groups. The null hypothesis that every group has the same survival function. The expected number of subjects surviving at each time point in each group is adjusted for the number of subjects at risk in the groups at each event time. The log-rank test determines if the observed number of events in each group is significantly different from the expected number. The formal test is based on a chi-squared statistic. The log-rank statistic has a chi-squared distribution with one degree of freedom, and the p-value is calculated using the chi-squared distribution. When the p-value is smaller than 0.05, it typically indicates that those groups differ significantly in survival times.

B. Survival analysis on real-world data

Tables S7-10 display the log-rank p-values for survival analysis of 13 TCGA major cancer types using different molecular data type: mRNA expression, microRNA expression, protein expression, and somatic copy number alterations (SCNAs); and different clustering methods. The p-values that are smaller than 0.05 are displayed in bold face. We found that for each single molecular data type our ECC method yields more significant p-values than other clustering methods. Table S11 displays the log-rank p-values for survival analysis of 13 TCGA major cancer types using pan-omics data (i.e. integrating mRNA expression, microRNA expression, protein expression, and SCNAs) and our ECC method. (Note that the competitive clustering methods cannot handle missing values or incomplete basic partitions, hence we only show the result of ECC on the pan-omics data.) We find that for each cancer type the p-value is smaller than 0.05, suggesting that by integrating 4 different molecular data types ECC generated significant subtypes for all the 13 cancer types.

bioRxiv preprint doi: https://doi.org/10.1101/073189; this version posted September 3, 2016. The copyright holder for this preprint (which was not certified by peer review) is the author/funder. All rights reserved. No reuse allowed without permission.

[S1] Schaffter, T., Marbach, D. & Floreano, D. Genenetweaver: in silico benchmark generation and performance profiling of network inference methods. *Bioinformatics* **27**, 2263–2270 (2011).

[S2] Souto, M., Costa, I., de Araujo, D., Ludermir, T. & Schliep, A. Clustering cancer gene expression data: a comparative study. *BMC bioinformatics* **9**, 1–14 (2008).

[S3] Banerjee, A., Merugu, S., Dhillon, I. & Ghosh, J. Clustering with bregman divergences. *Journal of Machine Learning Research* **6**, 1705–1749 (2005).

[S4] Liu, H., Wu, J., Tao, D., Zhang, Y. & Fu, Y. Dias: A disassemble-assemble framework for highly sparse text clustering. In *Proceedings of SIAM International Conference on Data Mining* (2015).

[S5] Klein, D. G. K. M. *Survival Analysis: A Self-Learning Text* (Springer, 2005).

[S6] Cancer Genome Atlas Research Network. Comprehensive molecular characterization of urothelial bladder carcinoma. *Nature* **507**, 315–322 (2014).

[S7] Cancer Genome Atlas Research Network. Comprehensive molecular portraits of human breast tumours. *Nature* **490**, 61–70 (2012).

[S8] Cancer Genome Atlas Research Network. Comprehensive molecular characterization of human colon and rectal cancer. *Nature* **487**, 330–337 (2012).

[S9] Cancer Genome Atlas Research Network. Comprehensive genomic characterization of head and neck squamous cell carcinomas. *Nature* **517**, 576–582 (2015).

[S10] Cancer Genome Atlas Research Network. Comprehensive molecular characterization of clear cell renal cell carcinoma. *Nature* **499**, 43–49 (2013).

[S11] Brat, D. & et al. Comprehensive, integrative genomic analysis of diffuse lower-grade gliomas. *The New England journal of medicine* **372**, 2481–2498 (2015).

[S12] Cancer Genome Atlas Research Network. Comprehensive molecular profiling of lung adenocarcinoma. *Nature* **511**, 543–550 (2014).

[S13] Cancer Genome Atlas Research Network. Comprehensive genomic characterization of squamous cell lung cancers. *Nature* **489**, 519–525 (2012).

[S14] Cancer Genome Atlas Research Network. Integrated genomic analyses of ovarian carcinoma. *Nature* **474**, 609–615 (2011).

[S15] Cancer Genome Atlas Research Network. The molecular taxonomy of primary prostate cancer. *Cell* **163**, 1011–1025 (2015).

[S16] Cancer Genome Atlas Research Network. Genomic classification of cutaneous melanoma. *Cell* **161**, 1681–1696 (2015).

[S17] Cancer Genome Atlas Research Network. Integrated genomic characterization of papillary thyroid carcinoma. *Cell* **159**, 676–690 (2014).

[S18] Cancer Genome Atlas Research Network. Integrated genomic characterization of endometrial carcinoma. *Nature* **497**, 67–73 (2013).

bioRxiv preprint doi: https://doi.org/10.1101/073189; this version posted September 3, 2016. The copyright holder for this preprint (which was not certified by peer review) is the author/funder. All rights reserved. No reuse allowed without permission.

TABLE SI. Notations for Supplementary Note 1

Symbol	Domain	Description
n	$\mathbf{Z}$	the number of subjects
m	$\mathbf{Z}$	the number of genes
r	$\mathbf{Z}$	the number of basic partitions
$\mathcal{X}$	$\mathbf{R}^{n\times m}$	the gene expression data matrix
π_v	$\{1,2,\cdots,K\}^n$	the v-th basic partition
K_v	$\mathbf{Z}$	the cluster number of π_v
π	$\{1,2,\cdots,K\}^n$	the consensus partition
K	$\mathbf{Z}$	the cluster number of π
B	$0,1^{n\times\sum_{v=1}^{r}K_v}$	the binary matrix for clustering
m_k	$\mathbf{R}^{\sum_{v=1}^{r}K_v}$	the k-th centroid matrix

TABLE SII. Notations for Supplementary Note 2

Symbol	Domain	Description
n	$\mathbf{Z}$	the number of genes in the network
F_i^{mRNA}	$\mathbf{R}$	the changing rate of mRNA concentration
F_i^{Prot}	$\mathbf{R}$	the changing rate of protein concentration
m_i	[0,1]	the maximum transcription rate
r_i	[0,1]	the translation rate
$\lambda_i^{\mathrm{mRNA}}$	$\mathbf{R}$	mRNA degradation rate
$\lambda_i^{\mathrm{Prot}}$	$\mathbf{R}$	protein degradation rate
$f_i(\cdot)$	[0,1]	the activation function of gene i
k_{ij}	$\mathbf{R}$	the dissociation constant
h_{ij}	[1,10]	the Hill coefficient
α_i	$\mathbf{R}$	the relative activation in state S_0
ρ	$\mathbf{R}$	the cooperativity factor
η_v, η_d, η_{ω_i}	$\mathbf{R}$	independent Gaussian white-noise process
c_1	(0,1)	molecular noise level
c_2	(0,1)	measurement noise level
N	$\mathbf{Z}$	the number of samples
p	$\mathbf{Z}$	the number of knock-out genes

TABLE SIII. Some key characteristics of 35 benchmark datasets for cluster validity

No	Dataset	Tissue	#Subject	#Genes	#Class	No	Dataset	Tissue	#Subject	#Genes	#Class
1	Alizadeh-2000-v1	Blood	42	1095	2	19	Lapointe-2004-v2	Prostate	110	2496	4
2	Alizadeh-2000-v2	Blood	62	2093	3	20	Liang-2005	Brain	37	1411	3
3	Alizadeh-2000-v3	Blood	62	2093	4	21	Nutt-2003-v1	Brain	50	1377	4
4	Armstrong-2002-v1	Blood	72	1081	2	22	Nutt-2003-v2	Brain	28	1070	2
5	Armstrong-2002-v2	Blood	72	2194	3	23	Nutt-2003-v3	Brain	22	1152	2
6	Bhattacharjee-2001	Lung	203	1543	5	24	Pomeroy-2002-v1	Brain	34	857	2
7	Bitter-2000	Skin	38	2201	2	25	Pomeroy-2002-v2	Brain	42	1379	5
8	Bredel-2005	Brain	50	1739	3	26	Ramaswamy-2001	Multi-tissue	190	1363	14
9	Chen-2002	Liver	179	85	2	27	Risinger-2003	Endometrium	42	1771	4
10	Chowdary-2006	Multi-tissue	104	182	2	28	Shipp-2002	Blood	77	798	2
11	Dyrskjot-2003	Bladder	40	1203	3	29	Singh-2002	Prostate	102	339	2
12	Garber-2001	Lung	66	4553	4	30	Su-2001	Multi-tissue	174	1571	10
13	Golub-1999-v1	Bone marrow	72	1868	2	31	Tomlins-2006-v1	Prostate	92	1288	4
14	Golub-1999-v2	Bone marrow	72	1868	3	32	Tomlins-2006-v2	Prostate	104	2315	5
15	Gordon-2002	Lung	181	1626	2	33	West-2001	Breast	49	1198	2
16	Khan-2001	Multi-tissue	83	1069	4	34	Yeoh-2002-v1	Bone marrow	248	2526	2
17	Laiho-2007	Colon	37	2202	2	35	Yeoh-2002-v2	Bone marrow	248	2526	6
18	Lapointe-2004-v1	Prostate	69	1625	3						

bioRxiv preprint doi: https://doi.org/10.1101/073189; this version posted September 3, 2016. The copyright holder for this preprint (which was not certified by peer review) is the author/funder. All rights reserved. No reuse allowed without permission.

TABLE SIV. Some key characteristics of 13 real-world datasets from TCGA

No	Database	#Class	protein		miRNA		mRNA		SCNA	
			#Instance	#protein	#Instance	#miRNA	#Instance	#mRNA	#Instance	#SCNA
1	BLCA [6]	4	127	190	328	1046	326	20531	330	24952
2	BRCA [7]	4	742	190	728	1046	1065	20531	1067	24952
3	COAD [8]	4	330	190	242	1046	292	20531	450	24952
4	HNSC [9]	4	212	190	471	1046	502	20531	508	24952
5	KIRC [10]	4	454	190	247	1046	523	20531	524	24952
6	LGG [11]	3	258	190	441	1046	445	20531	443	24952
7	LUAD [12]	3	237	190	441	1046	496	20531	502	24952
8	LUSC [13]	4	195	190	317	1046	476	20531	479	24952
8	OV [14]	4	408	190	474	1046	262	20531	575	24952
10	PRAD [15]	7	161	190	414	1046	418	20531	418	24952
11	SCKM [16]	4	206	190	416	1046	436	20531	438	24952
12	THCA [17]	5	370	190	503	1046	502	20531	503	24952
13	UCEC [18]	4	394	190	393	1046	162	20531	527	24952

Note: the cluster number is obtain from the original papers which publish the datasets.

bioRxiv preprint doi: https://doi.org/10.1101/073189; this version posted September 3, 2016. The copyright holder for this preprint (which was not certified by peer review) is the author/funder. All rights reserved. No reuse allowed without permission.

bioRxiv preprint doi: https://doi.org/10.1101/073189; this version posted September 3, 2016. The copyright holder for this preprint (which was not certified by peer review) is the author/funder. All rights reserved. No reuse allowed without permission.

TABLE SV. Performance of different clustering algorithms on benchmark datasets by R_n

No	Dataset	AL	SL	CL	KM	SC	LCE	ASRS	ECC
1	Alizadeh-2000-v1	0.0047	0.0000	0.0047	0.1856	0.1633	0.4981	0.4306	**0.5576**
2	Alizadeh-2000-v2	**0.8519**	-0.0427	0.7483	0.5241	0.5059	0.4100	0.4091	0.4093
3	Alizadeh-2000-v3	0.4387	-0.0129	0.3848	0.3917	0.3892	0.3235	**0.4615**	0.4464
4	Armstrong-2002-v1	-0.0451	-0.0138	**0.4753**	0.2356	0.2680	0.2102	0.2384	0.2296
5	Armstrong-2002-v2	0.0009	0.0007	0.4620	0.5690	0.5876	0.7821	0.7747	**0.8480**
6	Bhattacharjee-2001	0.2606	0.0390	**0.4662**	0.2173	0.1962	0.2040	0.2441	0.2362
7	Bitter-2000	0.0000	0.0000	-0.0103	-0.0144	-0.0157	0.0179	0.0179	**0.0429**
8	Bredel-2005	0.0056	0.0056	0.3671	0.3606	0.2933	0.3270	**0.5183**	0.3766
9	Chen-2002	-0.0031	-0.0031	-0.0065	0.2571	-0.0065	0.5365	-0.006	**0.6505**
10	Chowdary-2006	0.0091	0.0091	0.0091	0.0657	0.0091	0.5273	0.0657	**0.8857**
11	Dyrskjot-2003	0.0534	0.0534	0.0534	0.5069	0.5563	0.5779	0.5077	**0.6213**
12	Garber-2001	-0.0161	-0.0161	0.1023	0.1766	**0.1776**	0.0722	0.1558	0.1084
13	Golub-1999-v1	0.2313	0.0243	0.5016	0.5646	0.6860	0.6347	0.5905	**0.8473**
14	Golub-1999-v2	0.1710	0.0138	0.2440	0.5456	0.5758	0.6709	**0.8776**	0.8127
15	Gordon-2002	-0.0086	-0.0086	-0.0882	-0.0618	-0.0168	-0.0583	-0.0948	**-0.0126**
16	Khan-2001	-0.0126	-0.0152	0.1848	0.2979	0.5388	0.2951	0.3394	**0.4433**
17	Laiho-2007	0.0838	0.1355	-0.1028	**0.1964**	0.1914	0.1914	0.1244	0.1284
18	Lapointe-2004-v1	0.0402	0.0402	0.0402	**0.1770**	0.1549	0.1037	0.1568	0.1295
19	Lapointe-2004-v2	0.0253	0.0130	0.0375	0.1196	0.0798	0.0968	0.1018	**0.1386**
20	Liang-2005	0.0497	-0.1529	0.1573	0.1551	0.1775	**0.1937**	0.1573	0.1573
21	Nutt-2003-v1	0.0008	0.0005	0.1232	0.3246	0.2956	0.2483	0.3562	**0.3766**
22	Nutt-2003-v2	0.0023	0.0000	0.1082	0.0314	0.0023	0.3055	0.0023	**0.4176**
23	Nutt-2003-v3	0.1020	0.1020	0.1020	0.6993	0.8153	0.8153	**1.0000**	0.8153
24	Pomeroy-2002-v1	-0.0645	**-0.0366**	-0.0459	-0.0513	-0.0459	-0.0459	-0.0459	-0.0468
25	Pomeroy-2002-v2	0.0975	0.1012	0.2549	0.4636	0.5353	0.4571	0.4748	**0.4979**
26	Ramaswamy-2001	-0.0021	-0.0029	0.0126	0.1241	0.2221	0.1782	0.1348	**0.2285**
27	Risinger-2003	-0.0272	-0.0108	-0.0640	0.1122	0.1088	0.1000	0.0989	**0.1212**
28	Shipp-2002	**-0.0325**	**-0.0325**	**-0.0325**	-0.0848	**-0.0325**	-0.0935	-0.1003	-0.0918
29	Singh-2002	**0.0269**	0.0008	**0.0269**	0.0259	0.0330	0.0047	0.0245	0.0044
30	Su-2001	0.1296	0.0337	0.1821	0.3831	0.4959	0.4007	0.4175	**0.4532**
31	Tomlins-2006-v1	0.0180	0.0122	0.0485	0.1643	0.1747	**0.1911**	0.1510	0.1305
32	Tomlins-2006-v2	0.0099	0.0099	0.3178	0.2845	0.2339	0.3369	**0.4154**	0.3726
33	West-2001	0.0001	-0.0016	0.0001	0.2834	0.0001	**0.3875**	**0.3875**	**0.3875**
34	Yeoh-2002-v1	-0.0063	-0.0063	-0.0063	0.3664	0.0846	0.8803	-0.0063	**0.9344**
35	Yeoh-2002-v2	-0.0011	-0.0011	-0.0011	0.1785	0.1933	0.1277	0.1866	**0.2376**
	Average	0.0684	0.0068	0.1445	0.2507	0.2465	0.3117	0.2734	**0.3684**

bioRxiv preprint doi: https://doi.org/10.1101/073189; this version posted September 3, 2016. The copyright holder for this preprint (which was not certified by peer review) is the author/funder. All rights reserved. No reuse allowed without permission.

TABLE SVI. Performance of different clustering algorithms on benchmark datasets by NMI

No	Dataset	AL	SL	CL	KM	SC	LCE	ASRS	ECC
1	Alizadeh-2000-v1	0.0939	0.0601	0.0939	0.1776	0.1369	0.4167	0.3516	**0.4940**
2	Alizadeh-2000-v2	**0.8119**	0.0342	0.6972	0.6454	0.6634	0.5672	0.5877	0.5832
3	Alizadeh-2000-v3	0.6421	0.0960	0.5665	0.5789	0.5930	0.5300	**0.6441**	0.6340
4	Armstrong-2002-v1	0.0631	0.0263	**0.4389**	0.3606	0.3793	0.3459	0.3622	0.3571
5	Armstrong-2002-v2	0.1311	0.0780	0.5536	0.6133	0.6243	0.7654	0.7460	**0.8154**
6	Bhattacharjee-2001	0.4039	0.1014	**0.5032**	0.4252	0.4504	0.4186	0.4941	0.4585
7	Bitter-2000	**0.0640**	**0.0640**	0.0000	0.0127	0.0083	0.0323	0.0323	0.0502
8	Bredel-2005	0.0848	0.0848	0.3685	**0.3809**	0.2916	0.3688	0.4769	0.3712
9	Chen-2002	0.0199	0.0199	0.0008	0.2058	0.0008	0.4980	0.0010	**0.6273**
10	Chowdary-2006	0.0459	0.0459	0.0459	0.1424	0.0459	0.4739	0.1424	**0.8098**
11	Dyrskjot-2003	0.1613	0.1613	0.1613	0.5124	0.5082	**0.5743**	0.5158	0.5584
12	Garber-2001	0.0734	0.0734	0.0999	0.1801	0.1689	0.1647	0.1294	**0.2025**
13	Golub-1999-v1	0.2764	0.0684	0.4837	0.5358	0.5809	0.6085	0.5536	**0.8149**
14	Golub-1999-v2	0.2868	0.0803	0.3496	0.5762	0.5429	0.6870	**0.8453**	0.7737
15	Gordon-2002	0.0083	0.0083	0.1168	0.1385	**0.1684**	0.1411	0.1099	0.1479
16	Khan-2001	0.0966	0.0941	0.4857	0.5149	**0.6718**	0.5109	0.5644	0.6221
17	Laiho-2007	0.0340	0.1680	0.0664	0.1479	**0.1959**	**0.1959**	0.0749	0.0768
18	Lapointe-2004-v1	0.0466	0.0466	0.0466	**0.1956**	0.1269	0.1101	0.1826	0.1281
19	Lapointe-2004-v2	0.0513	0.0406	0.0419	0.1620	0.1173	0.1357	0.1379	**0.1652**
20	Liang-2005	0.3002	0.1181	0.3545	**0.3811**	0.3597	0.3772	0.3545	0.3545
21	Nutt-2003-v1	0.1293	0.1296	0.2900	0.4742	0.4233	0.3844	**0.5083**	0.4994
22	Nutt-2003-v2	0.0406	0.0778	0.2513	0.0589	0.0406	0.3988	0.0406	**0.4021**
23	Nutt-2003-v3	0.1600	0.1600	0.1600	0.6545	0.7523	0.7523	**1.0000**	0.7523
24	Pomeroy-2002-v1	0.0521	0.0332	0.0079	0.0453	0.0079	0.0079	0.0079	**0.0092**
25	Pomeroy-2002-v2	0.4150	0.4177	0.5396	0.5935	0.6401	0.6032	0.5937	**0.6171**
26	Ramaswamy-2001	0.2176	0.1608	0.3376	0.5203	0.5172	0.5126	**0.5560**	0.5277
27	Risinger-2003	0.1349	0.1203	0.1877	0.2867	0.2744	0.2784	0.2709	**0.2911**
28	Shipp-2002	0.0288	0.0288	0.0288	0.0747	0.0288	0.1235	0.1124	**0.1280**
29	Singh-2002	0.0675	0.0360	**0.0675**	0.0475	0.0562	0.0101	0.0342	0.0100
30	Su-2001	0.4919	0.2874	0.5088	0.6018	**0.6614**	0.6122	0.6422	0.6276
31	Tomlins-2006-v1	0.1281	0.1058	0.1574	0.2849	0.2533	**0.3257**	0.3065	0.2558
32	Tomlins-2006-v2	0.1158	0.1158	0.4676	0.4653	0.3586	0.5050	**0.5815**	0.5266
33	West-2001	0.0823	0.0530	0.0823	0.2603	0.0823	**0.3125**	**0.3125**	**0.3125**
34	Yeoh-2002-v1	0.0070	0.0070	0.0070	0.3342	0.0366	0.7968	0.0070	**0.8564**
35	Yeoh-2002-v2	0.0691	0.0691	0.0691	0.3760	0.3309	0.2768	**0.4175**	0.3815
	Average	0.1667	0.0935	0.2468	0.3419	0.3171	0.3949	0.3628	**0.4355**

bioRxiv preprint doi: https://doi.org/10.1101/073189; this version posted September 3, 2016. The copyright holder for this preprint (which was not certified by peer review) is the author/funder. All rights reserved. No reuse allowed without permission.

TABLE SVII. Survival analysis of different clustering algorithms on protein expression data.

Dataset	#cluster	AL	SL	CL	KM	SC	LCE	ASRS	ECC
BLCA	4	0.8400	0.6230	0.3210	**0.0241**	**0.0005**	0.0881	0.1030	**0.0212**
BRCA	4	0.2660	**0.0008**	0.0988	0.0997	0.1130	0.3060	0.1460	**0.0313**
COAD	4	0.8750	0.9530	0.8430	**0.0157**	0.0738	**1.20E-8**	**4.82E-5**	**3.32E-9**
HNSC	4	0.7540	**0.0050**	0.5520	0.7340	0.5110	0.9840	0.5960	0.1820
KIRC	4	0.7640	0.9140	0.2460	0.4120	0.6560	0.1680	0.7590	**0.0313**
LGG	3	**0.0182**	**0.0305**	**0.0002**	0.0563	0.0198	**0.0094**	0.1780	**0.0016**
LUAD	3	0.3730	0.8350	0.3220	0.4790	0.3990	**0.0293**	0.5070	**0.0245**
LUSC	4	0.9050	0.9290	0.9340	0.6670	0.6050	0.6550	0.5420	0.1980
OV	4	0.8090	0.5450	0.1900	**0.0275**	**0.0446**	**0.0485**	**0.0327**	**0.0021**
PRAD	7	**1.19E-6**	**9.78E-7**	**3.16E-6**	**0.0011**	0.0918	0.8140	**0.0124**	**0.0020**
SCKM	4	0.0848	0.2860	**0.0100**	0.0929	**0.0411**	**0.0381**	**0.0059**	**0.0035**
THCA	5	0.2380	**0.0255**	0.3470	0.1910	0.1480	0.0799	0.1370	**0.0138**
UCEC	4	0.4530	**3.00E-8**	0.9860	0.9860	0.4550	0.8450	0.3700	0.1310
#Significance		2	6	3	4	3	5	4	**10**

Note: the values in the table represent the p-value of log-rank test.

TABLE SVIII. Survival analysis of different clustering algorithms on miRNA expression data.

Dataset	#cluster	AL	SL	CL	KM	SC	LCE	ASRS	ECC
BLCA	4	0.2780	0.5880	0.5940	0.0616	0.5620	0.3410	0.2400	**0.0124**
BRCA	4	0.3110	0.6350	0.5410	**1.53E-5**	0.0717	**3.97E-6**	**1.12E-7**	**6.37E-8**
COAD	4	0.3290	0.6430	0.2070	0.2290	0.1960	**8.88E-4**	**0.0246**	**5.91E-4**
HNSC	4	0.8900	0.8820	0.7650	0.5760	0.6770	0.0605	**4.45E-5**	**0.0090**
KIRC	4	0.7970	0.6420	0.0692	0.2180	**0.0093**	**0.0180**	0.1090	**0.0223**
LGG	3	0.8820	0.9640	0.8940	0.9850	0.9000	0.7450	0.0640	0.0751
LUAD	3	0.8350	0.1200	0.7410	0.2870	0.3580	**0.0038**	0.8260	**0.0028**
LUSC	4	0.1060	0.3450	0.0565	**0.0152**	**0.0394**	0.1310	0.3120	**0.0442**
OV	4	0.5540	**0.0007**	0.2410	0.6290	0.4190	0.2340	0.2340	**0.0375**
PRAD	7	0.4570	0.4250	0.6500	0.3330	0.3200	0.8720	0.6270	0.1840
SCKM	4	0.0619	0.6870	0.4920	0.6390	0.6940	0.0663	0.0575	**0.0076**
THCA	5	0.4660	**0.0064**	**0.0053**	0.0892	0.1100	**0.0119**	**0.0157**	**3.75E-4**
UCEC	4	0.5280	0.4570	0.6290	0.6870	0.6080	0.5530	0.3520	0.2680
#Significance		0	2	1	2	2	5	4	**10**

Note: the values in the table represent the p-value of log-rank test.

bioRxiv preprint doi: https://doi.org/10.1101/073189; this version posted September 3, 2016. The copyright holder for this preprint (which was not certified by peer review) is the author/funder. All rights reserved. No reuse allowed without permission.

TABLE SIX. Survival analysis of different clustering algorithms on mRNA expression data.

Dataset	#cluster	AL	SL	CL	KM	SC	LCE	ASRS	ECC
BLCA	4	**1.06E-7**	**8.88E-8**	**1.06E-7**	**0.0258**	0.6860	0.1280	0.0938	**0.0187**
BRCA	4	**5.35E-3**	0.1740	**0.0401**	0.1760	0.0840	0.5980	**0.0155**	**0.0011**
COAD	4	0.8930	0.8960	0.8720	**0.0163**	**0.0296**	**0.0048**	0.0743	**0.0008**
HNSC	4	0.2950	**8.53E-5**	0.1350	0.7470	0.5440	0.6290	0.1440	0.1160
KIRC	4	**0.0025**	**0.0012**	**0.0036**	0.0612	0.1450	0.2420	0.1550	**0.0314**
LGG	3	**0.0156**	**0.0156**	**0.0155**	0.1270	0.1230	0.2650	**0.0023**	**0.0039**
LUAD	3	**0.0109**	0.8290	0.3190	**0.0429**	**0.0034**	**0.0189**	**0.0157**	**0.0028**
LUSC	4	0.0990	0.2100	**0.0241**	**0.0355**	0.4740	0.0769	0.1360	**0.0258**
OV	4	0.2210	**4.92E-10**	0.1700	0.6360	0.3780	0.8720	0.7660	0.2210
PRAD	7	**4.29E-9**	**4.49E-9**	**5.88E-9**	**7.29E-11**	**4.10E-9**	**0.0070**	**6.75E-13**	**8.59E-6**
SCKM	4	**0.0012**	**0.0012**	**0.0015**	0.5230	**0.0006**	0.1350	**5.91E-10**	**3.94E-6**
THCA	5	**0.0147**	0.5650	0.0713	**0.0244**	0.0561	0.2380	0.0710	**0.0024**
UCEC	4	0.5790	0.0594	0.1930	0.1850	0.2460	0.3670	0.4890	0.1240
#Significance		8	7	7	6	4	3	5	**10**

Note: the values in the table represent the p-value of log-rank test.

TABLE SX. Survival analysis of different clustering algorithms on SCNA data.

Dataset	#cluster	AL	SL	CL	KM	SC	LCE	ASRS	ECC
BLCA	4	0.3710	0.3710	0.3810	0.6340	0.3580	0.4340	0.3800	0.1910
BRCA	4	0.6540	0.6540	0.1160	**0.0090**	0.4790	0.0798	0.3520	**0.0375**
COAD	4	0.9320	0.9320	0.9010	0.1600	0.7920	0.7670	0.4660	0.2340
HNSC	4	**0.0003**	**0.0003**	**0.0380**	0.5280	0.5730	0.8280	0.7710	0.3800
KIRC	4	0.6580	0.7510	0.0929	0.4390	0.1060	0.2690	0.3710	0.1730
LGG	3	0.8800	0.9950	0.6430	0.5710	0.6130	0.8750	0.9740	0.4130
LUAD	3	0.5420	0.5420	0.5880	0.0763	0.2390	**0.0121**	**0.0080**	**0.0067**
LUSC	4	0.8900	0.8190	0.3870	0.3560	0.3810	0.1710	0.5540	**0.0425**
OV	4	0.7500	0.7500	0.1270	0.1710	0.0904	0.1730	0.1380	**0.0359**
PRAD	7	0.8410	**2.40E-7**	0.5060	0.2640	**0.0008**	**0.0160**	**0.0046**	**0.0007**
SCKM	4	0.8730	0.8140	0.6790	0.5660	0.1970	0.2210	0.2040	**0.0491**
THCA	5	0.1530	0.5180	0.1440	0.2670	0.1960	0.1360	0.5440	0.1080
UCEC	4	0.1100	0.1100	0.2310	**0.0484**	0.0673	0.4860	0.3450	0.1260
#Significance		1	2	1	2	1	2	2	**6**

Note: the values in the table represent the p-value of log-rank test.

bioRxiv preprint doi: https://doi.org/10.1101/073189; this version posted September 3, 2016. The copyright holder for this preprint (which was not certified by peer review) is the author/funder. All rights reserved. No reuse allowed without permission.

TABLE SXI. Survival analysis of ECC on pan-omics data.

Dataset	#cluster	ECC	Dataset	#cluster	ECC	Dataset	#cluster	ECC
BLCA	4	**0.0027**	BRCA	4	**0.0131**	COAD	4	**8.69E-6**
HNSC	4	**0.0323**	KIRC	4	**0.0010**	LGG	3	**0.0119**
LUAD	3	**2.87E-5**	LUSC	4	**0.0393**	OV	4	**0.0008**
PRAD	7	**0.0006**	SCKM	4	**0.0131**	THCA	5	**0.0035**
UCEC	4	**0.0043**						

Note: the values in the table represent the p-value of log-rank test.

bioRxiv preprint doi: https://doi.org/10.1101/073189; this version posted September 3, 2016. The copyright holder for this preprint (which was not certified by peer review) is the author/funder. All rights reserved. No reuse allowed without permission.

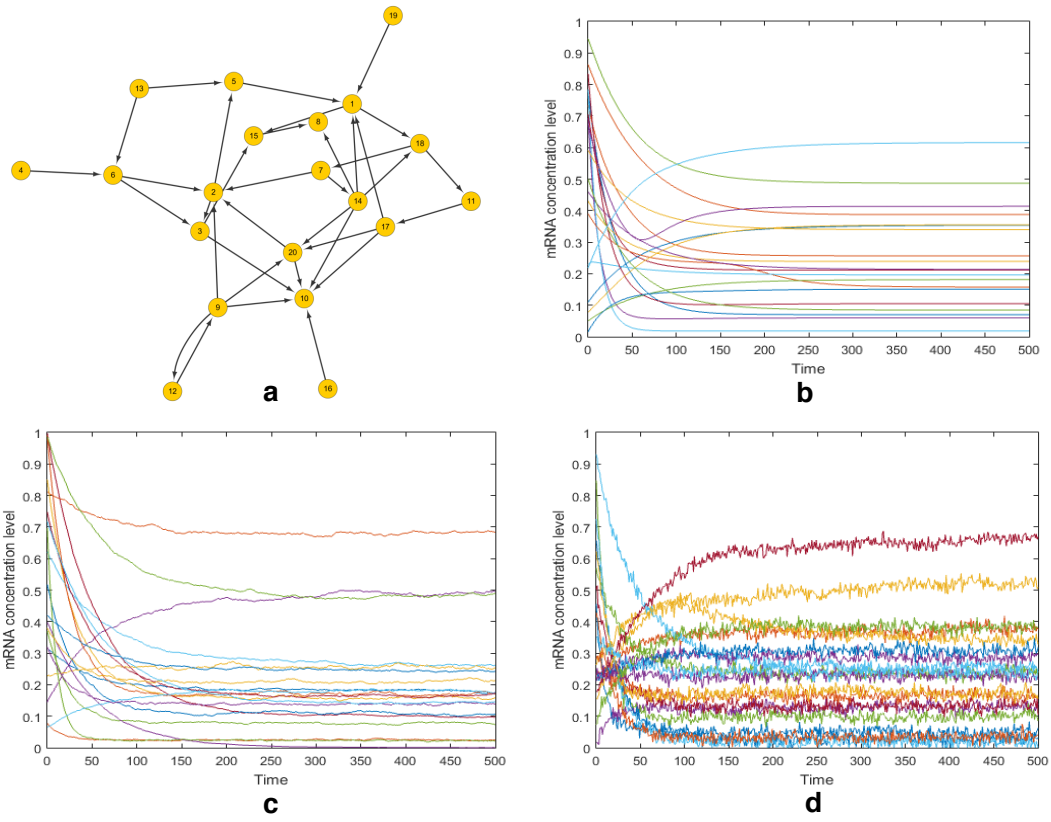

Figure S1. The random regulatory network of 20 genes and the time evolutions of mRNA concentration level. **a** represents the gene regulatory network of 20 genes, which is generated randomly with the mean in-degree of 2. **b** depicts the time evolution of mRNA concentration level without noise. The initial states are randomly generated. Each curve represents the time evolution of mRNA concentration level of a certain gene node. **c** depicts the time evolution of mRNA concentration level with molecular noise level = 0.01. **d** depicts the time evolution of mRNA concentration level with molecular noise level = 0.01, measurement noise level = 0.012. Each line represents the time evolution of mRNA concentration level of a gene node. It is easy to find that the time evolution curve without noise is smooth, while the time evolution with noise as a stochastic process is rough.

bioRxiv preprint doi: https://doi.org/10.1101/073189; this version posted September 3, 2016. The copyright holder for this preprint (which was not certified by peer review) is the author/funder. All rights reserved. No reuse allowed without permission.

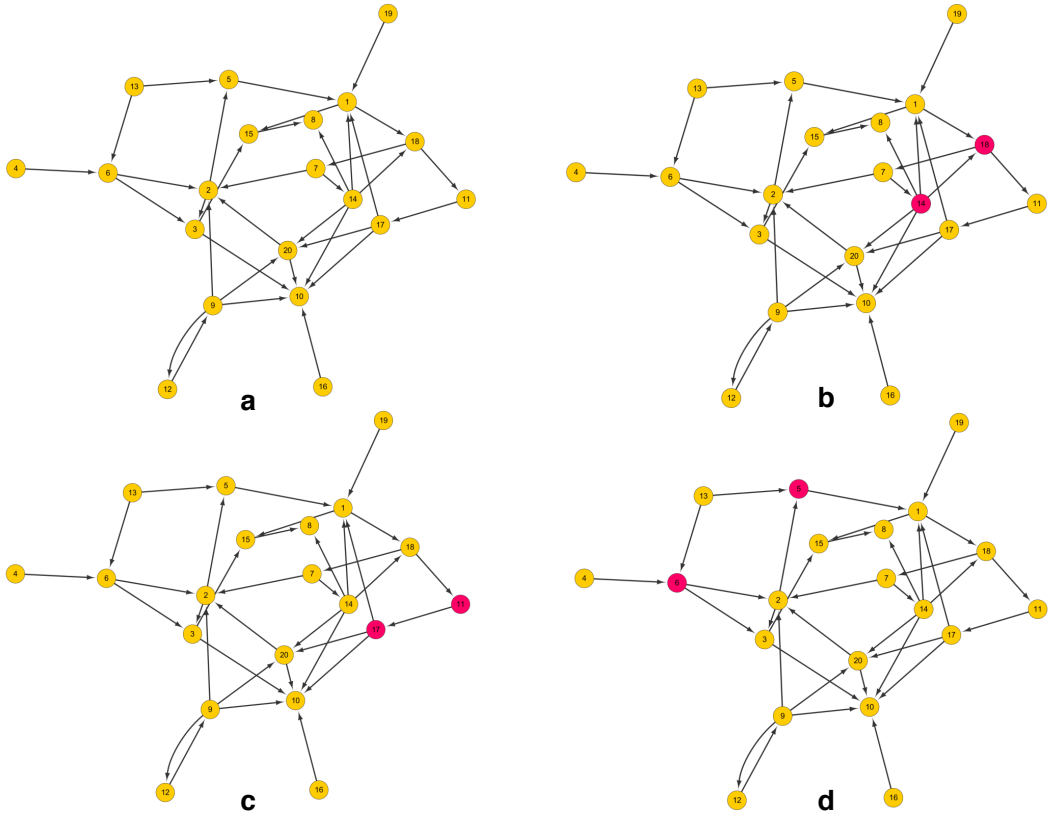

Figure S2. Normal gene regulatory network and three subtypes. **a** illustrates the normal gene regulatory network of 20 genes. **b** illustrates subtype 1 with two randomly knock-out genes. **c** illustrates subtype 2 with two randomly knock-out genes. **d** illustrates subtype 3 with two randomly knock-out genes.

bioRxiv preprint doi: https://doi.org/10.1101/073189; this version posted September 3, 2016. The copyright holder for this preprint (which was not certified by peer review) is the author/funder. All rights reserved. No reuse allowed without permission.

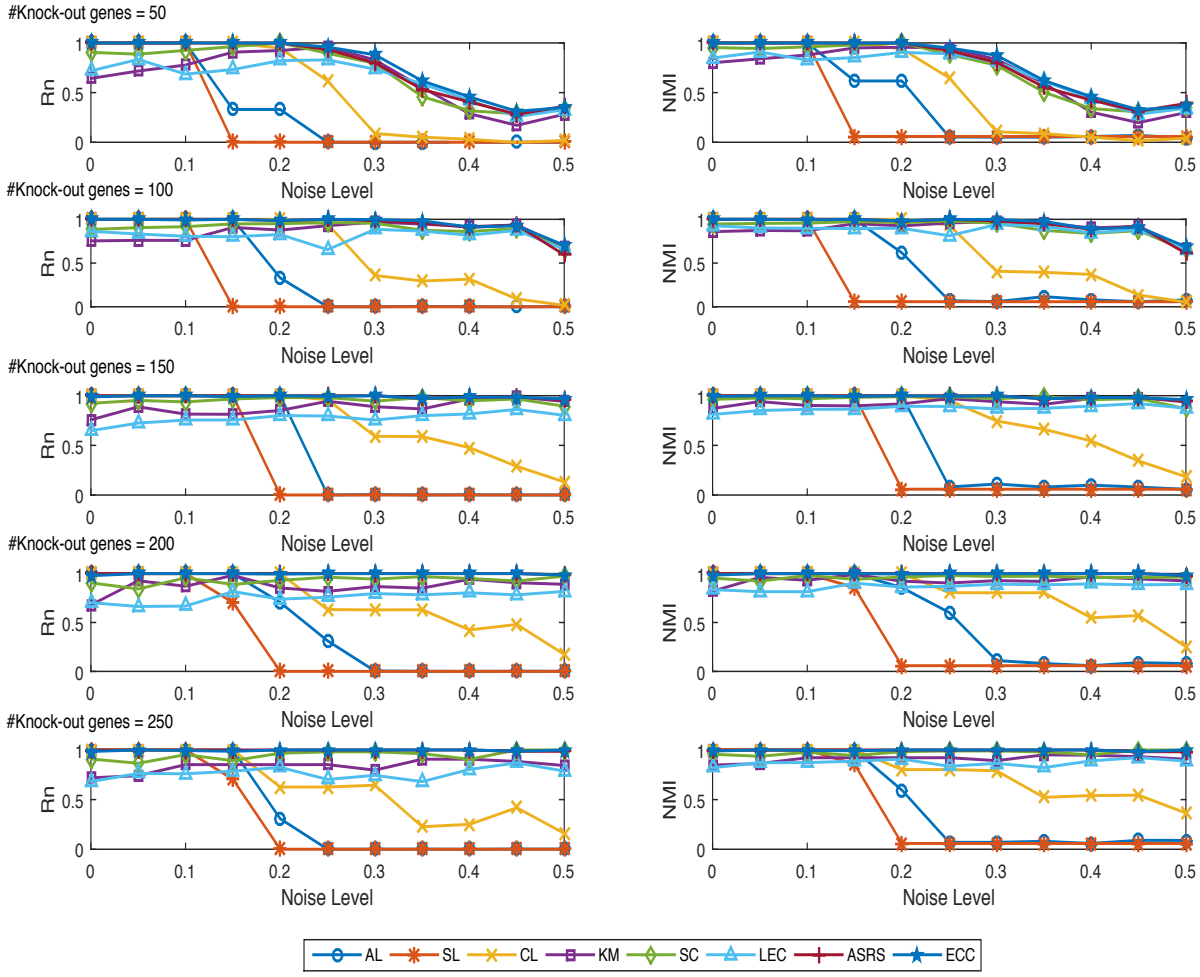

Figure S3. Performance of different clustering algorithms on the 55 synthetic datasets (based on an Erdös-Rényi random gene regulatory network of 500 genes). ECC has substantial advantages over other methods on the datasets marked by blue pentagram lines.

bioRxiv preprint doi: https://doi.org/10.1101/073189; this version posted September 3, 2016. The copyright holder for this preprint (which was not certified by peer review) is the author/funder. All rights reserved. No reuse allowed without permission.

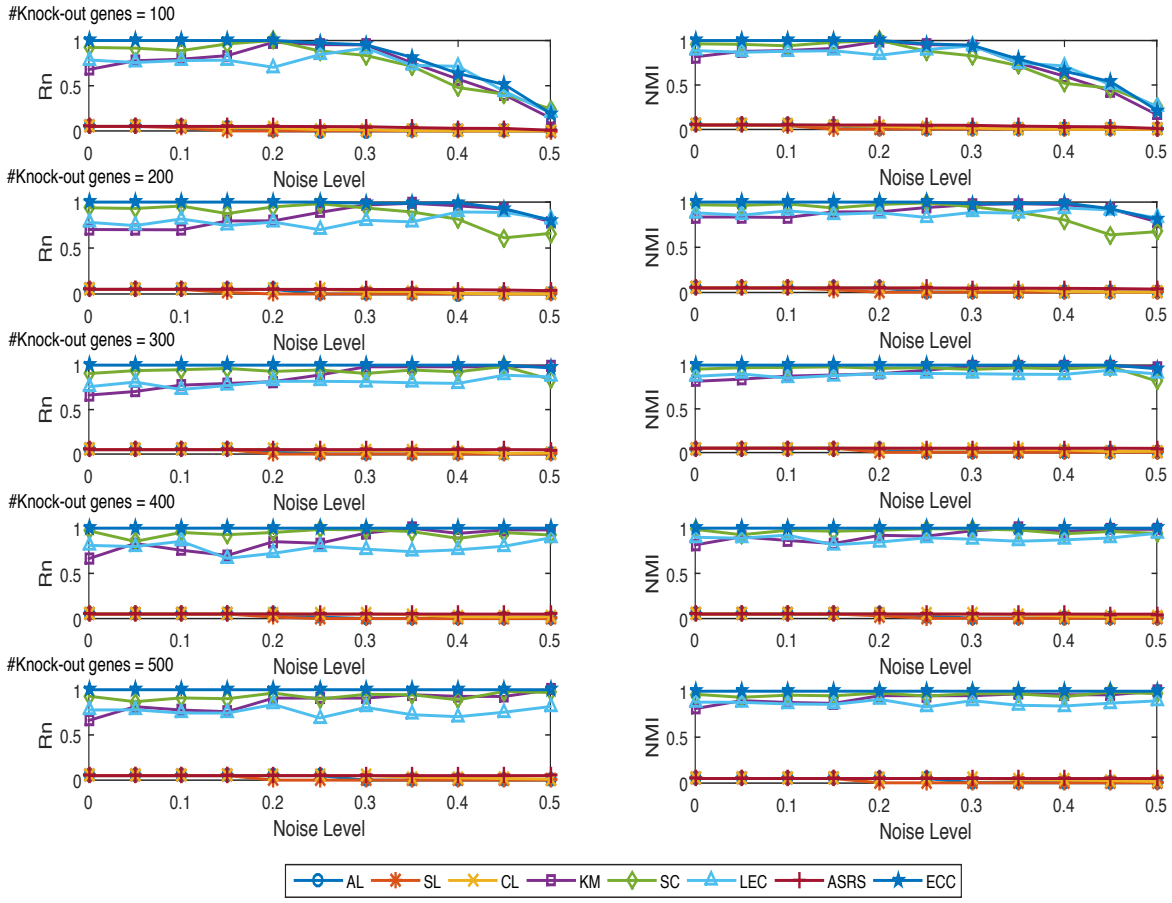

Figure S4. Performance of different clustering algorithms on the 55 synthetic datasets (based on a real human transcriptional regulation network of 2723 genes). ECC has substantial advantages over other methods on the datasets marked by blue pentagram lines.

bioRxiv preprint doi: https://doi.org/10.1101/073189; this version posted September 3, 2016. The copyright holder for this preprint (which was not certified by peer review) is the author/funder. All rights reserved. No reuse allowed without permission.

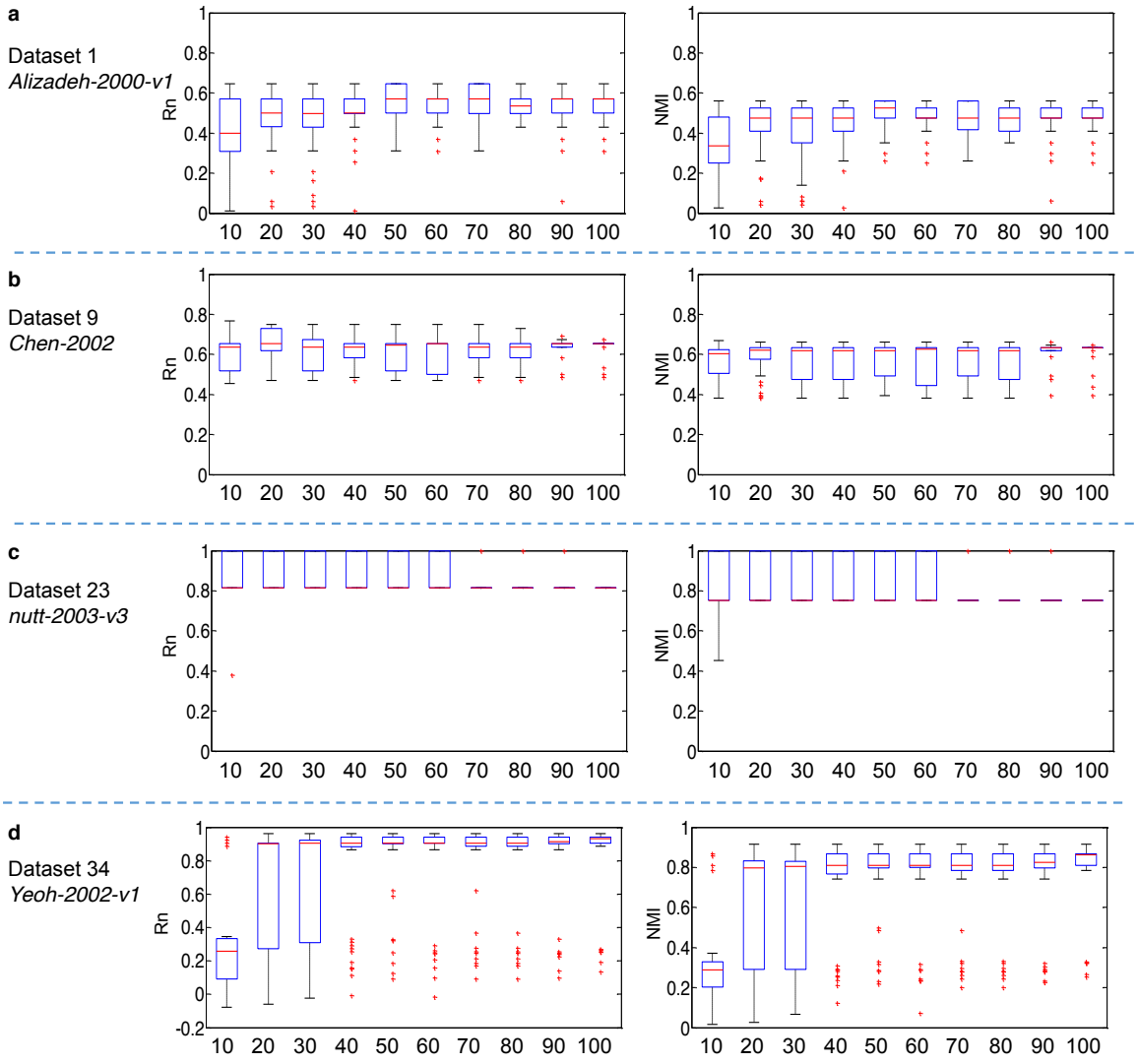

Figure S5. Impact of different numbers of basic partitions on ECC. The x-axis denotes the number of basic partitions. For each scenario, ECC runs 100 times for the boxplot. As the increase of basic partitions, the performance goes up and the variance becomes narrower and narrower.

bioRxiv preprint doi: https://doi.org/10.1101/073189; this version posted September 3, 2016. The copyright holder for this preprint (which was not certified by peer review) is the author/funder. All rights reserved. No reuse allowed without permission.

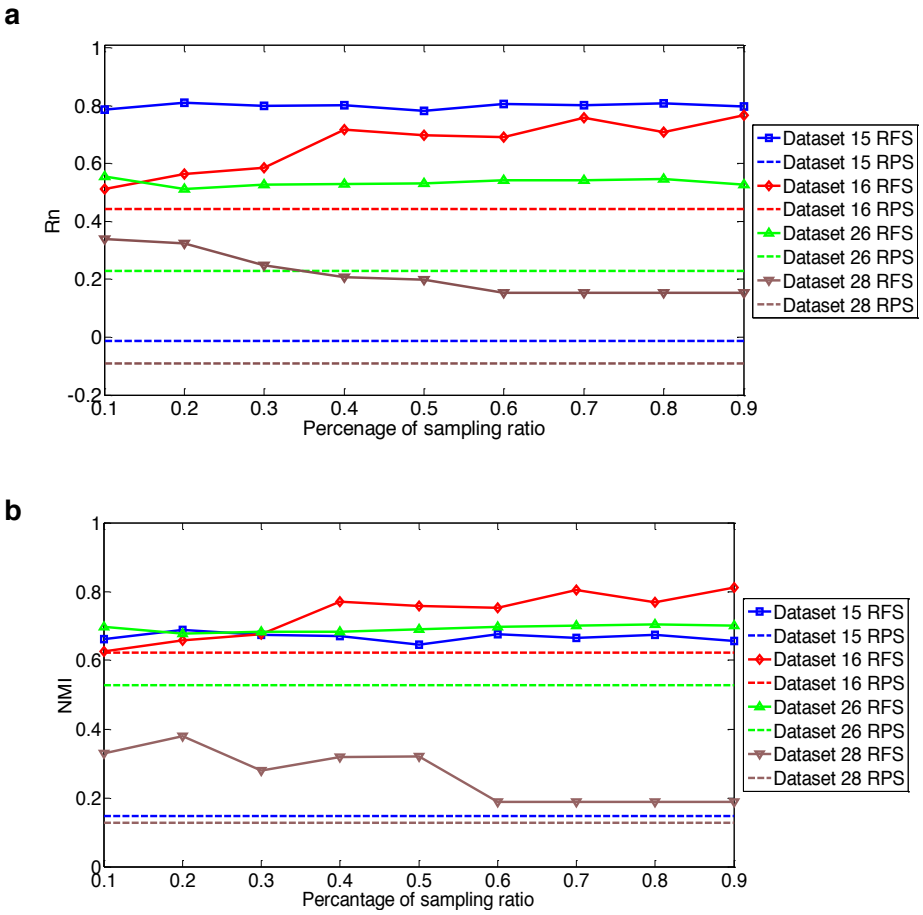

Figure S6. Random feature selection (RFS) strategies with different sampling ratios on ECC. On these four datasets, the performance of RFS exceeds those of RPS with all sampling ratios, which indicates that RFS can help to avoid noisy and irrelevant genes. Although it is difficult to select discriminative genes for cluster analysis, ECC can fuse the partial knowledge from RFS to achieve promising results.

bioRxiv preprint doi: https://doi.org/10.1101/073189; this version posted September 3, 2016. The copyright holder for this preprint (which was not certified by peer review) is the author/funder. All rights reserved. No reuse allowed without permission.

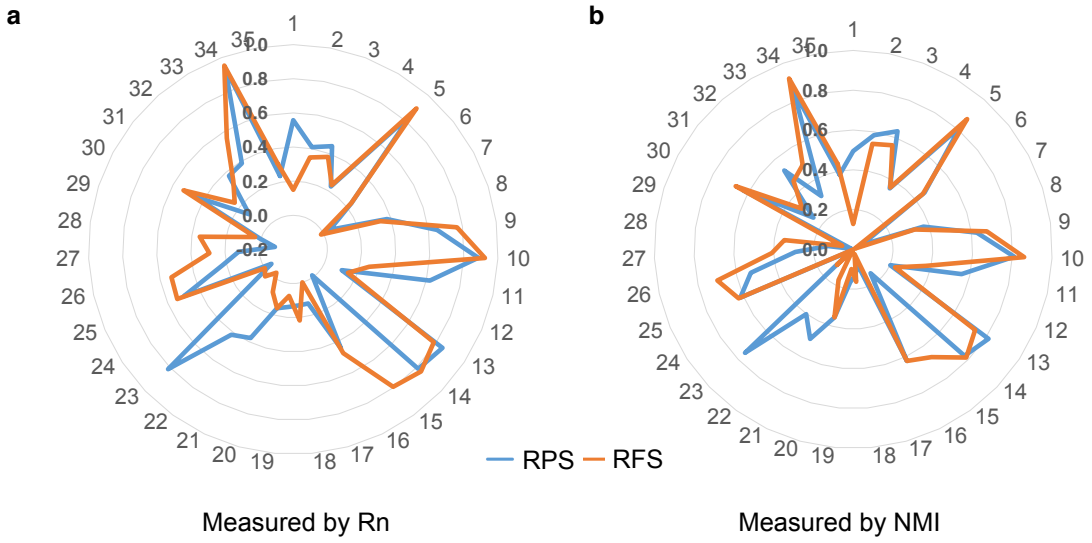

Figure S7. Comparison of different basic partition generation strategies on ECC. In RPS strategy, we apply K-means with the cluster number varying from 2 to $\sqrt{n}$. In RFS strategy, we apply K-means to 10% sampling ratio of the genes. RPS is suitable for the datasets which contain some potential sub-clusters, while RFS is suitable for the datasets containing noisy and irrelevant genes.

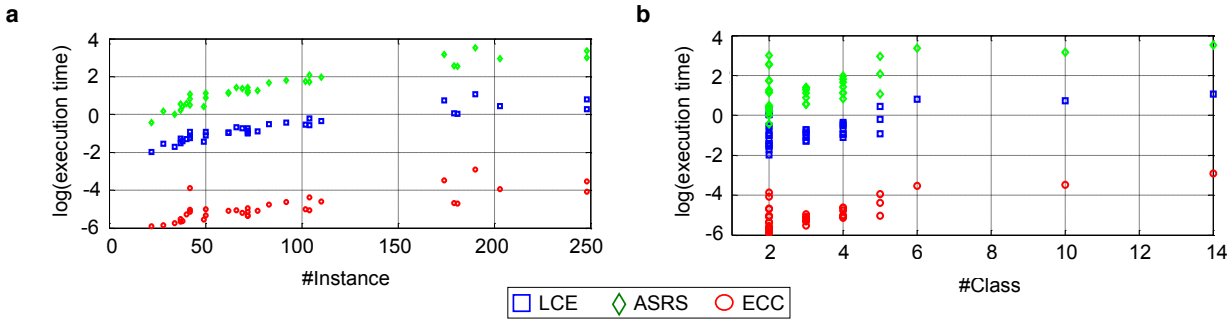

Figure S8. Execution time of three different consensus clustering methods. **a** shows the logarithm of the execution time in terms of the number of subjects and **b** shows the the logarithm of the execution time in terms of the cluster number. From these figures, ECC shows dramatically merits over two other consensus clustering methods (LCE and ASRS) in terms of efficiency. From the scope of these scatter plots, we can see that the time complexity of ECC is linear the number of subjects and the cluster number, while LCE and ASRS suffer from $\mathcal{O}(n^2 \log n)$ and $\mathcal{O}(n^3)$, respectively. This indicates ECC is suitable for large-scale gene expression data analysis.

bioRxiv preprint doi: https://doi.org/10.1101/073189; this version posted September 3, 2016. The copyright holder for this preprint (which was not certified by peer review) is the author/funder. All rights reserved. No reuse allowed without permission.

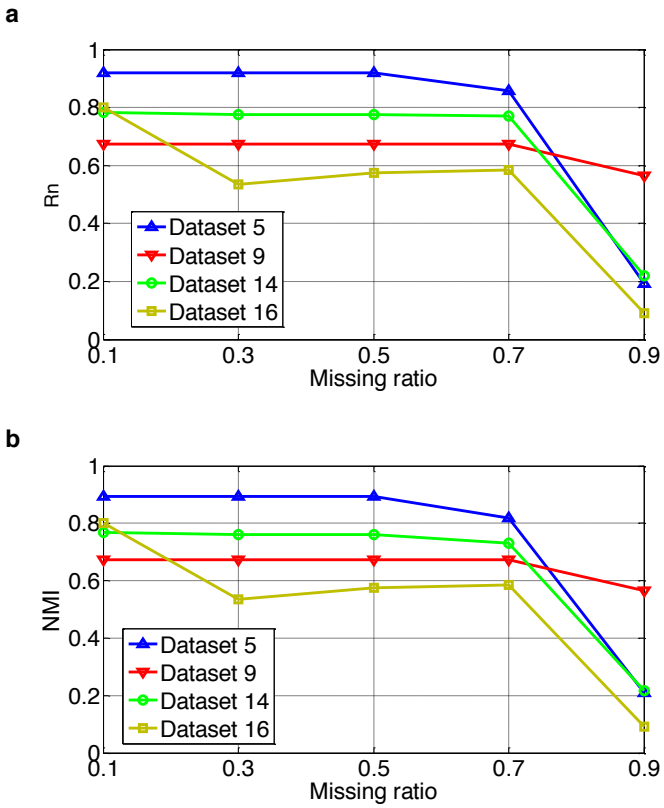

Figure S9. Performance of ECC with different missing ratios on 4 datesets. To generate incomplete basic partitions, we randomly remove some instances and employ K-means to assign the rest instances from 1 to K, where K is the user-defined cluster number. For these unsampled instances, the labels are assigned to be 0. The above process are repeated $r = 100$ times and we employ ECC to fuse these IBPs into a consensus one.